 Accepted Manuscript published as REP-19-0293.R2. Accepted for publication: 18-Nov-2019

Blastocyst transfer in mice alters the placental transcriptome and growth

Katerina Menelaou[1,2], Malwina Prater[2], Simon J. Tunster[1,2], Georgina E.T. Blake[1,2], Colleen Geary Joo[3], James C. Cross[4], Russell S. Hamilton[2,5], and Erica D. Watson[1,2,*]

[1]Department of Physiology, Development, and Neuroscience, University of Cambridge, Cambridge, UK

[2]Centre for Trophoblast Research, University of Cambridge, Cambridge, UK

[3]Transgenic Services, Clara Christie Centre for Mouse Genomics, University of Calgary, Calgary, Canada

[4]Department of Comparative Biology and Experimental Medicine, University of Calgary, Calgary, Canada

[5]Department of Genetics, University of Cambridge, Cambridge, UK

*Corresponding author: E.D.W., Department of Physiology, Development, and Neuroscience, University of Cambridge, Physiological Laboratory, Downing Street, Cambridge, CB2 3EG, UK; email: edw23@cam.ac.uk

SHORT TITLE: Embryo transfer alters placenta transcriptome

KEYWORDS: epigenetic regulation, histone modifications, assisted reproductive technologies, trophoblast, fetal growth

WORD COUNT: 6503 words

ABSTRACT

Assisted reproduction technologies (ART) are becoming increasingly common. Therefore, how these procedures influence gene regulation and feto-placental development are important to explore. Here, we assess the effects of blastocyst transfer on mouse placental growth and transcriptome. C57Bl/6 blastocysts were transferred into uteri of B6D2F1 pseudopregnant females and dissected at embryonic day 10.5 for analysis. Compared to non-transferred controls, placentas from transferred conceptuses weighed less even though the embryos were larger on average. This suggested a compensatory increase in placental efficiency. RNA-sequencing of whole male placentas revealed 543 differentially expressed genes (DEGs) after blastocyst transfer: 188 and 355 genes were down-regulated and up-regulated, respectively. DEGs were independently validated in male and female placentas. Bioinformatic analyses revealed that DEGs represented expression in all major placental cell types and included genes that are critical for placenta development and/or function. Furthermore, the direction of transcriptional change in response to blastocyst transfer implied an adaptive response to improve placental function to maintain fetal growth. Our analysis revealed that CpG methylation at regulatory regions of two DEGs was unchanged in female transferred placentas and that DEGs had fewer gene-associated CpG islands (within ~20 kb region) compared to the larger genome. These data suggested that altered methylation at proximal promoter regions might not lead to transcriptional disruption in transferred placentas. Genomic clustering of some DEGs warrants further investigation of long-range, cis-acting epigenetic mechanisms including histone modifications together with DNA methylation. We conclude that embryo transfer, a protocol required for ART, significantly impacts the placental transcriptome and growth.

 Accepted Manuscript published as REP-19-0293.R2. Accepted for publication: 18-Nov-2019

INTRODUCTION

More than seven million babies worldwide have been born using some form of assisted reproduction technology (ART) largely as a treatment approach to infertility (European Society of Human Reproduction and Embryology (ESHRE), 2018 February 18. *ART Fact Sheet*. Retrieved from https://www.eshre.eu/. Grimbergen, Belgium). ART includes a range of procedures with varying degrees of invasiveness (e.g., superovulation, *in vitro* fertilisation (IVF), intracytoplasmic sperm injection, embryo culture, embryo biopsy, gamete and embryo vitrification, and blastocyst transfer). While ART is generally safe, growing evidence suggests that individuals born using these technologies are at an increased risk of intrauterine growth restriction, perinatal complications (Quinn & Fujimoto 2016), and/or developing cardiovascular disease later in life (Tararbit *et al.* 2013, Valenzuela-Alcaraz *et al.* 2013, Liu *et al.* 2015, Guo *et al.* 2017). Since optimal placental function is required for normal fetal growth and development, it is predicted that placenta pathologies are responsible for some of the adverse pregnancy outcomes associated with ART (Delle Piane *et al.* 2010, Thomopoulos *et al.* 2013, Choux *et al.* 2015). Indeed, ART pregnancies were overrepresented in the highest quartile of placental weight and underrepresented in the highest quartile of birthweight (Haavaldsen *et al.* 2012).

To explore the effects of ART on placental structure and function, animal models have been utilised. Similar to humans, the mouse placentation site is composed of three major layers: the outer maternal layer, which includes decidual cells of the uterus, maternal immune cells, and the maternal vasculature that brings blood to and from the implantation site; the metabolic ‘junctional’ region, containing many endocrine cells and which attaches the placenta to the uterus through the invasion of trophoblast cells; and an inner layer composed of highly branched villi required for nutrient, gas, and waste exchange between maternal and fetal circulations (Watson & Cross 2005). Defects in placenta development and/or function have repercussions for fetal growth and health

(Watson & Cross 2005, Perez-Garcia *et al.* 2018). IVF and/or superovulation in mice are associated with large placentas with reduced vascular density and altered nutrient transport at late gestation to produce normal-sized or growth-restricted fetuses (Delle Piane *et al.* 2010, Bloise *et al.* 2012, Weinerman *et al.* 2017). Indeed, sub-optimally formed placentas might undergo counter-balancing mechanisms leading to adaptive responses (Choux *et al.* 2015). How and when this dialogue occurs is unclear.

The mechanism through which ART influences the formation and function of the maternal-fetal interface is not well understood. The vast majority of studies have focused on CpG methylation of imprinted genomic loci (Khosla *et al.* 2001, Mann *et al.* 2004, Fortier *et al.* 2008, Rivera *et al.* 2008, de Waal *et al.* 2014, Fauque *et al.* 2010, Wang *et al.* 2010, Bloise *et al.* 2012). Genomic imprinting is an epigenetic phenomenon in mammals whereby a small number of genes are expressed in a parent-of-origin-specific manner, a process that is regulated by DNA methylation. Many imprinted genes are expressed in the placenta and are important for its development and function (Tunster *et al.* 2013). Directed analysis of imprinted regions can act as a convenient read-out of functional DNA methylation changes across the genome (Padmanabhan *et al.* 2013). Therefore, studies showing altered DNA methylation at imprinted loci after ART hypothesize that these technologies might influence the establishment of DNA methylation genome-wide with consequences for placental cell differentiation (Choux *et al.* 2015). Dysregulation of other epigenetic mechanisms (e.g., histone modifications, non-coding RNA expression) are largely unstudied in the context of ART.

One procedure that all ART have in common is the transfer of the blastocyst into the uterus of a recipient female. While many ART studies in mice have taken into account the potential effects of blastocyst transfer (Kholsa *et al.* 2001, Delle Piane *et al.* 2010, Fauque *et al.* 2010, Bloise *et al.* 2012), the impact of this procedure alone on placentation site growth and transcription is not well understood. Here, we show that blastocyst transfer

 Accepted Manuscript published as REP-19-0293.R2. Accepted for publication: 18-Nov-2019

in mice has a stark impact on transcriptional regulation and likely influences placental efficiency even as the placenta matures. Furthermore, our genome-wide approach enabled us to determine that changes in DNA methylation at proximal promoter regions may not cause transcriptional disruption. Therefore, a long-range study of cis-acting epigenetic mechanisms in addition to DNA methylation is required.

MATERIALS AND METHODS

Mice

C57Bl/6 conceptuses were generated by natural mating of C57Bl/6 mice at 7-10 weeks of age. No hormones were used. [C57Bl/6 x DBA/2] F1 hybrid (B6D2F1) female mice were mated at 7-10 weeks of age with vasectomized C57Bl/6 males to generate a pseudopregnant state. B6D2F1 mice have 50% genetic similarity to C57Bl/6 mice and were used because C57Bl/6 females are notoriously poor recipients for blastocyst transfer. A broad range of genetic backgrounds has been used for donor and recipient mice across ART studies (Mann et al. 2004, Fortier *et al.* 2008, Piane *et al.* 2010, Wang *et al.* 2010, Chen et al. 2015), including hybrid recipient females as in our study (Kholsa *et al.* 2001, Fauque *et al.* 2010, Bloise *et al.* 2012). C57Bl/6 conceptuses that were derived by natural mating and did not undergo the transfer process were used as controls. Noon of the day that the copulatory plug was detected was considered embryonic (E) day 0.5. Mice were euthanized via cervical dislocation. All experiments were performed in accordance with the Canadian Council on Animal Care and the University of Calgary Committee on Animal Care (protocol number M06109). This research was also regulated under the Animal (Scientific Procedures) Act 1986 Amendment Regulations 2012 following ethical review by the University of Cambridge Animal Welfare and Ethical Review Body.

125

126 ***Blastocyst transfers***

127 Conceptuses from the blastocyst transfer experiment were generated as previously
128 described (Padmanabhan *et al.* 2013). Briefly, using M2 media (Sigma-Aldrich, Gillingham,
129 UK), embryos were flushed at E3.25 from the oviducts and uteri of C57Bl/6 females.
130 Embryos were cultured in KSOM media (Millipore, Etobicoke, Canada) microdrops
131 covered in mineral oil (Millipore) at 37°C for no more than 30 minutes. This unavoidable
132 culture period allowed for the surgical preparation of the recipient female. Embryos were
133 transferred by injection into the oviducts of pseudopregnant B6D2F1 recipients 2.5 days
134 after mating them with vasectomized C57Bl/6 males. Litters were never pooled.

135

136 ***Dissections and phenotyping***

137 All conceptuses were dissected at E10.5. For transferred litters, the timing of dissection
138 corresponded to the staging of the recipient female (Ueda *et al.* 2003). Implantation sites
139 were dissected away from the uterine myometrium in cold 1x phosphate buffered saline.
140 Embryos and placentas were rigorously scored for gross phenotypes (see below and
141 Padmanabhan *et al.* 2013), photographed, weighed, and snap frozen in liquid nitrogen for
142 storage at -80°C. Similar to other ART studies on mouse placenta (Fauque *et al.* 2010,
143 Wang *et al.* 2010, Fortier *et al.* 2008, Rivera *et al.* 2008, Bloise *et al.* 2012), whole
144 placentas including the mesometrial decidua were assessed. Retaining the decidua is
145 important for sample consistency since reliably removing the decidua without influencing
146 parietal trophoblast giant cell (TGC) numbers is difficult. It also contains invading
147 trophoblast cells (Simmons *et al.* 2008) that are important to assess.

148 For phenotype scoring, defective embryo growth was determined by assessing
149 crown-rump length and somite pairs. Crown-rump lengths that were greater or less than
150 two standard deviations from the mean crown-rump length of C57Bl/6 controls were

 Accepted Manuscript published as REP-19-0293.R2. Accepted for publication: 18-Nov-2019

151 distinguished as growth enhancement or restriction, respectively. Somite staging was
152 determined according to e-Mouse Atlas Project (http://www.emouseatlas.org): 30-39
153 somite pairs were considered the normal range for E10.5 and somite pairs <30 indicated
154 developmental delay. Embryos were also assessed for the appearance of hemorrhage,
155 resorptions, twinning, and congenital malformations including defective neural tube
156 closure, abnormal heart loop directionality, and/or presence of pericardial edema or heart
157 enlargement. Placentas were grossly scrutinized for the presence and orientation of
158 chorioallantoic attachment and hemorrhage. Sex of conceptuses was determined by
159 polymerase chain reaction (PCR) genotyping of yolk sac DNA using reported methods
160 (Chuma & Nakatsuji 2001, Tunster 2017). Images were obtained using a Zeiss SteREO
161 Discovery V8 microscope with an AxioCam MRc5 camera and AxioVision 4.7.2 software
162 (Carl Zeiss Ltd, Cambridge, UK).
163
164 ***RNA and DNA extraction***
165 Whole placentas were homogenized using lysing matrix D beads (MP Biomedicals,
166 Carlsbad, USA). For quantitative reverse transcription-PCR (qRT-PCR) analysis, total
167 RNA was extracted using TRIzol reagent (Sigma-Aldrich) according to the manufacturer's
168 instructions. For methylation analysis, DNA and RNA were extracted using the AllPrep
169 DNA/RNA kit (QIAGEN, Manchester, UK). All RNA extracts were treated with DNAse I
170 (Thermo Scientific, Waltham, USA).
171
172 ***Transcriptome analysis***
173 RNA libraries were prepared from whole placentas of non-transferred and transferred
174 C57Bl/6 conceptuses at E10.5. Four male placentas taken from 3-4 litters were assessed
175 per experimental group. Placentas chosen for analysis were associated with
176 phenotypically normal embryos (i.e., the embryos displayed normal crown-rump lengths

and somite pair counts, and were absent of congenital malformations). Library preparation and sequencing was performed by Cambridge Genomic Services, Department of Pathology, University of Cambridge. The concentration and purity of RNA was determined by a SpectroStar spectrophotometer (BMG LABTECH, Aylesbury, UK) and an Agilent Tapestation Bioanalyzer (Aligent Technologies LDA UK Ltd, Stockport, UK) determined RNA integrity. Libraries were prepared using 200 ng of total RNA and TruSeq stranded mRNA Library Preparation kit (Illumina, Chesterford, UK). A unique index sequence was added to each RNA library to allow for multiplex sequencing. Libraries were pooled and sequenced on the Illumina NextSeq500 platform with 75-base-pair single-end reads. Sequencing was performed in duplicate to provide >18 million reads per sample. To monitor sequencing quality control, 1% PhiX Control (Illumina) spike-in was used. Quality control of Fastq files was performed using FastQC and fastq_screen. Sequences were trimmed with Trim Galore! and aligned to GRCm38 mouse genome using STAR aligner. Alignments were processed using custom ClusterFlow (v0.5dev) pipelines and assessed using MultiQC (0.9.dev0). Gene quantification was determined with HTSeq-Counts (v0.6.1p1). Additional quality control was performed with rRNA and mtRNA counts script, feature counts (v 1.5.0-p2) and qualimap (v2.2). Differential gene expression was performed with DESeq2 package (v1.22.2, R v3.5.2). Read counts were normalised on the estimated size factors. Principle component analysis was performed on the rlog transformed count data for the top 5,000 most variable genes. Heatmaps were generated with ‘ComplexHeatmap' R package (v 1.20.0). Karyoplots were generated with karyoploteR (v1.8.8).

Data availability

 Accepted Manuscript published as REP-19-0293.R2. Accepted for publication: 18-Nov-2019

The RNA-sequencing data is accessible through ArrayExpress EMBL-EBI accession number E-MTAB-8036. All code to reproduce the bioinformatics analysis are freely available from https://github.com/CTR-BFX/2019-Menelaou-Watson.

Quantitative reverse transcription-PCR (qRT-PCR)

Primers were designed using NCBI Primer-BLAST software (Ye *et al.* 2012). For primer sequences, refer to **Supplementary table 1**. Reverse transcription reactions were performed with the RevertAid H Minus reverse transcriptase (Thermo Scientific) and random hexamer primers (Thermo Scientific) using 1 µg of total RNA according to manufacturer's instructions. PCR amplification was performed using MESA SYBR Green qPCR MasterMix Plus (Eurogentec, Liege, Belgium) on a DNA Engine Opticon2 thermocycler (BioRad, Hercules, USA). Transcript levels were normalised to *Polr2a* RNA and analysed using the comparative Ct method. cDNA levels in C57Bl/6 control placentas were normalised to 1. For qRT-PCR validation of the RNA-seq experiment, 4-7 whole male or female placentas were analysed per experimental group from 2-4 litters, and were independent of those assessed by RNA-seq. Experiments were conducted in technical triplicates.

Bisulfite pyrosequencing

Genomic DNA was bisulphite converted using the Imprint DNA Modification Kit (Sigma-Aldrich) using the one-step modification procedure. Pyrosequencing assays were designed using PyroMark Assay Design SW 2.0 software (QIAGEN). For primer sequences, refer to **Supplementary table 1**. PCR was performed in triplicate using HotStarTaq DNA polymerase (QIAGEN) and 5 ng of bisulphite-converted DNA with the following PCR conditions: 95°C for 5 minutes followed by 95°C for 30 seconds, 56°C for 30 seconds and 72°C for 55 seconds for 40 cycles, then 72°C for 5 minutes. PCR products

were bound to Streptavidin Sepharose High Performance beads (GE Healthcare, Chicago, USA) and purified by sequential washing in 70% ethanol, 0.4 mol/L NaOH and 10 mmol/L Tris-acetate (pH 7.6) using a Pyromark Q96 Vacuum Prep Workstation (QIAGEN). The purified product was mixed with the pyrosequencing primer in annealing buffer (20 mmol/L Tris-acetate pH 7.6, 2 mmol/L magnesium acetate), incubated at 85°C for 4 minutes then at room temperature for 4 minutes. Pyrosequencing was conducted using PyroMark Gold reagents (QIAGEN) on a PyroMark MD pyrosequencer (QIAGEN). Analysis of methylation status was performed using Pyro Q-CpG 1.0.9 software (Biotage, Hengoed, UK). The mean CpG methylation was calculated using five whole female placentas from 3-4 litters and at least two technical replicates per experimental group.

Statistical Analysis

Statistical analyses were performed using GraphPad Prism 6 software (La Jolla, USA). Parametric data (e.g., litter sizes, crown-rump lengths, placenta weights, weight ratios) were analysed using *t* tests. Relative risks were determined to compare males and females of each phenotypic group, and p-values were calculated using Fisher's exact test. For the RNA-sequencing data, the nbinomTest was used in R to calculate the p-value and p-adjusted value of differentially expressed genes (DEGs). For mRNA expression, data was analysed using Mann-Whitney tests or *t* tests with Welch correction where appropriate. Pyrosequencing data was analysed using *t* tests when primers spanned a single CpG site and two-way ANOVA with Sidak's multiple comparisons test when primers spanned two or more CpG sites. Frequency of CpG repeats was determined using Fisher's exact test. $P<0.05$ was considered significant.

Software and online resources

Graphs were generated using GraphPad Prism 6 software. DEGs were subject to

 Accepted Manuscript published as REP-19-0293.R2. Accepted for publication: 18-Nov-2019

enrichment analysis using Enrichr (http://amp.pharm.mssm.edu/Enrichr/) (Chen *et al.* 2013a, Kuleshov *et al.* 2016). Placental gene expression was determined using the Mouse Encode Project (http://www.mouseencode.org/) (Yue *et al.* 2014) and Mouse Cell Atlas (http://bis.zju.edu.cn/MCA/) (Han *et al.* 2018). Some phenotype data was obtained from Deciphering the Mechanisms of Developmental Disorders database (https://dmdd.org.uk), which is funded by the Wellcome Trust (www.wellcome.ac.uk) with support from the Francis Crick Institute (www.crick.ac.uk) and is licensed under a Creative Commons Attribution license (https://creativecommons.org/licenses/by/4.0/legalcode). CpG islands were identified with the University of California, Santa Cruz (UCSC) Mouse Genome Browser (http://genome.ucsc.edu/) using NCBI37/mm9 mouse genome assembly of the C57Bl/6 genome (Haeussler *et al.* 2019). CpG island tracks were defined as a stretch of DNA between 200-1300 bp with a GC content >50% and a ratio of observed:expected CpG dinucleotides >0.6. The enhancer-promoter units (EPUs) were generated according to previously published data (Shen *et al.* 2012). For this analysis, UCSC Mouse Genome Browser (http://genome.ucsc.edu/) using NCBI37/mm9 mouse genome assembly of the C57Bl/6 genome (Haeussler *et al.* 2019) was used to determine CpG island tracks and to analyse C57Bl/6 placenta histone modification peaks from the ENCODE ChIP-seq data set (GEO accession: GSM1000133, GSM1000134) (ENCODE Project Consortium 2012, Yue *et al.* 2014). The NCBI37/mm9 coordinates were lifted over to GRCm38/mm10 using LiftOver tool from UCSC. To generate an intersect between DEGs (log2fc1) and EPUs, bedtools2 (v2.26.0) software was used. Random gene lists were generated using Random Gene Set Generator (www.molbiotools.com).

RESULTS

Blastocyst transfer potentially leads to increased placental efficiency at E10.5

To better understand how blastocyst transfer affects fetoplacental development, we mated

C57Bl/6 female mice (N=10) without superovulation to C57Bl/6 males (N=10). Pre-implantation embryos were flushed at E3.25 from oviducts and uteri of donor females and transferred into oviducts of pseudopregnant B6D2F1 females. Transferred blastocysts were allowed to implant and were dissected at E10.5 (staged according to recipient females (Ueda *et al.* 2003)) for phenotyping. C57Bl/6 control conceptuses were derived from natural matings, did not undergo the blastocyst transfer procedure, and were dissected at E10.5 for similar analyses.

Prior to transfer, litter sizes at E3.25 ranged between 7-10 embryos and included compact morula- and blastocyst-staged embryos (**Table 1**). Two litters contained at least one embryo with an abnormal appearance (**Table 1**). However, all embryos were transferred regardless of appearance. Ten pseudopregnant B6D2F1 females received embryos but only eight were pregnant at E10.5 (80% efficiency). The average implantation rate was 47.2% when all transferred litters were considered and 58.9% when only considering transfers that resulted in pregnancy. Thus, litter sizes in the blastocyst transfer group were significantly smaller (5.4 ± 0.5 implantation sites/litter; $p<0.001$) than control litters (9.5 ± 0.4 implantation sites/litter) (**Table 2**). No congenital malformations or gross placental phenotypes were apparent in control or transferred conceptuses at E10.5 (see methods, **Table 2**). However, one litter in the transfer group was developmentally delayed since the number of somite pairs in these embryos ranged between 16-22 pairs (**Fig. 1A**) instead of the expected 30-40 somite pairs. At E10.5, 20.9% of the transferred conceptuses were resorbed compared to only 5.3% of controls (**Table 2**). Although not statistically significant ($p=0.200$), this result suggested that blastocyst transfer might lead to increased post-implantation lethality before E10.5. A larger data set is required to explore this finding further.

Overall, male and female conceptuses were present in a 1:1 ratio at E10.5 in both control and transferred groups (**Table 2**) indicating that sex was not a selective factor on

 Accepted Manuscript published as REP-19-0293.R2. Accepted for publication: 18-Nov-2019

survival after blastocyst transfer. While average embryo weights were similar (**Fig. 1B**), placental weights were lower in transferred conceptuses compared to controls (**Fig. 1C**) suggesting that the blastocyst transfer protocol might alter placental development. Furthermore, embryo:placenta weight ratios were higher in transferred conceptuses, yet only significantly so in transferred female conceptuses (p=0.025; **Fig. 1D**).

To further define the growth phenotype, embryo crown-rump lengths were measured. While mean lengths were not significantly different between control and transfer groups (**Fig. 1E**), frequency distribution curves of crown-rump lengths were generated (**Fig. 1F**) to detect specific embryos with abnormal growth. Defective growth was defined as crown-rump lengths that were >2 standard deviations from the mean length of control embryos. Regardless of sex, a similar frequency of growth restriction was observed in control (4.4 – 4.5% of embryos) and transferred conceptuses at E10.5 (5.9% of embryos, p=0.687; **Fig. 1A,F, Table 2**). Interestingly, three out of 17 (17.6%) of the transferred male embryos displayed growth enhancement (**Fig. 1A,F, Table 2**). This frequency was not statistically significant (p=0.08), likely due to the small sample size. No transferred female embryos or control embryos were growth enhanced (**Fig. 1F, Table 2**) suggesting that this phenotype might be sexually dimorphic. A lack of correlation between litter size and crown-rump length in control or transferred litters at E10.5 (**Fig. 1G**) suggested that litter size is an unlikely confounder of this study.

When all phenotypes (e.g., growth restriction, growth enhancement, developmental delay) and resorptions were grouped together, fewer embryos were classified as 'phenotypically normal' (PN) in the transferred group (55.8%; p<0.001) compared to controls (91.6%; **Table 2**). When the analysis was restricted to conceptuses with PN embryos (**Fig. 1A,F**), average weight of the associated placentas remained lower in transferred conceptuses compared to controls, regardless of sex (p<0.004; **Fig. 1J**). Despite this, average embryo weight was normal in PN males (p=0.472) and higher in PN

females (p=0.019) compared to same-sex controls (**Fig. 1I**). These data suggested that the placentas of transferred conceptuses, though small, were potentially more efficient in both sexes. This hypothesis was reinforced by increased embryo:placenta weight ratios in PN transferred conceptuses (p<0.002; **Fig. 1K**). Future histological and functional analyses are required to confirm this hypothesis. Altogether, these data imply that after blastocyst transfer, normal growth trajectory of the embryo is likely reliant upon functional compensation by the placenta.

Blastocyst transfer alters the placental transcriptome at E10.5

Typically, large litters result in smaller conceptuses, particularly in late gestation when competition for maternal resources is highest (Ishikawa *et al.* 2006). In our data at E10.5, we observed that neither embryo crown-rump length (**Fig. 1G**) nor placenta weight (**Fig. 2A**) correlated with litter size. These data further demonstrate that litter size is an unlikely confounder in our study.

We sought to determine the effect of blastocyst transfer on the placental transcriptome. A genome-wide transcriptome analysis was performed via RNA-sequencing to determine differential mRNA expression in whole placentas from control (N=4) or transferred (N=4) C57Bl/6 conceptuses at E10.5. Since the placenta transcriptome is known to exhibit some sexual dimorphism (Gonzalez *et al.* 2018) and due to tissue availability, only male placentas associated with PN embryos were selected for analysis. cDNA libraries generated from placental RNA were sequenced using the NextSeq500 (Illumina) platform and bioinformatically analysed.

A principal component analysis revealed that, based on RNA content, the placentas of control and transferred conceptuses clustered separately (**Fig. 2B**). Differential mRNA expression was determined when log_2[fold change] >1 (i.e., fold change ≥2; p<0.05). Remarkably, 543 genes were differentially expressed in transferred placentas compared to

 Accepted Manuscript published as REP-19-0293.R2. Accepted for publication: 18-Nov-2019

controls including 355 up-regulated and 188 down-regulated genes (**Fig. 2C-D**). We selected 27 (5.0%) DEGs for validation via qRT-PCR using RNA isolated from independent whole male placentas (N=4-7 placentas/group) (**Fig. 2E-F, 4B**). Thirteen out of 17 genes that were down-regulated in the RNA-sequencing experiment were also down-regulated in the qRT-PCR analysis ($p<0.05$), with the remaining four genes showing a strong downward trend (**Fig. 2E, 4B**). Furthermore, eight out of 10 up-regulated genes were also statistically validated by qRT-PCR ($p<0.05$; **Fig. 2F, 4B**). Therefore, the RNA-sequencing experiment was deemed robust and reliable.

All major placental cell types represented by differentially expressed genes

To determine if blastocyst transfer affected gene expression in specific placental cell types, we performed an extensive literature and database search to resolve the spatial expression of the DEGs in mouse placentation sites. The primary resource for this analysis was a published single cell RNA-sequencing data set on whole C57Bl/6 mouse placentas at E14.5 (Han *et al.* 2018). Although the developmental stage assessed in Han *et al.* (2018) differed slightly from our analysis, the data can be used as a predictive indicator of spatial expression.

Of the 543 DEGs that were identified, placental expression of the majority of DEGs (362 genes) is not currently described in mouse. Expression of 102 DEGs has been reported in the C57Bl/6 mouse placenta at term but without information about cell type specificity (Yue *et al.* 2014) (**Supplementary table 2**). Spatial expression of the remaining 79 genes has been characterized. In several cases (14 DEGs), gene expression occurred in more than one placental cell population (**Fig. 3A, Supplementary table 3**). Additionally, most cell types present in the mouse placentation site were represented by DEGs (e.g., trophoblast, endothelial, endoderm, stromal, decidual, hematopoietic lineages) (**Fig. 3A, Supplementary table 3**) further indicating that blastocyst transfer is unlikely to affect a

single cell lineage. A similar proportion of DEGs were detected in trophoblast cells (26/79 DEGs, 32.9%) and endodermal cells (27/79 DEGs, 34.2%), though fewer DEGs were detected in the decidua (19/79 DEGs, 24.1%) and fetal vascular endothelium (5/79, DEGs, 6.3%) (**Fig. 3A, Supplementary table 3**). It will be important in the future to validate the spatial expression of these genes in the mouse placentation site at E10.5 using in situ hybridisation. Overall, this result suggested that blastocyst transfer caused broad transcriptional changes throughout the mouse placentation site at midgestation even when the embryo was considered phenotypically normal.

DEGs were enriched for genes associated with placental growth and function

The primary annotation terms enriched in placentas from transferred conceptuses at E10.5 included genes important for placental development, growth and function (**Fig. 3B**). Enrichment groups included genes associated with specific mammalian phenotypes (e.g., decreased vascular permeability, abnormal visceral yolk sac, abnormal lipid and glucose homeostasis, and decreased circulating IGF1 and insulin levels), and genes required for specific biological processes (e.g., cell adhesion, response to decreased oxygen levels, and negative regulation of cell proliferation and growth) (**Fig. 3B**). At least 13 DEGs identified are important for placental development and/or function as evidenced by gene knockout and over-expression studies (**Table 3**). Furthermore, 31 DEGs encode for proteins with nutrient transporter activity (24/31 [77.4%] DEGs were up-regulated; 7/31 [22.6%] DEGs were down-regulated) including gap junction protein 1 (*Gjb1*), and those important for lipid and fatty acid transport (*Slc27a2*, *Mttp*, *Apom*, *Amn*) and glutamate transport (*Slc17a8*, *Slc7a11*) (**Table 4**). Together, these data supported the hypothesis that blastocyst transfer results in structural and functional compensation by the placenta with the aim of maintaining embryo growth. Whether changes in gene expression lead to altered protein expression or activity in transferred placentas requires exploration.

 Accepted Manuscript published as REP-19-0293.R2. Accepted for publication: 18-Nov-2019

409

410 ***Dysregulation of DNA methylation at proximal promoter regions by blastocyst***
411 ***transfer is unlikely to disrupt transcription***

412 The mechanism by which blastocyst transfer alters gene expression is not well
413 understood, though epigenetic dysregulation has been implicated (Choux *et al.* 2015,
414 Canovas *et al.* 2017). To examine the potential sensitivity of the DEGs to changes in DNA
415 methylation, we first evaluated whether the top 50 down-regulated genes (fold change >
416 3.1) and top 50 up-regulated genes (fold change > 6.7) contained intragenic CpG islands
417 or proximal promoter CpG islands (within 20 kb of the gene) (**Fig. 4A**). This result was
418 compared to 50 randomly selected genes as a proxy for the rest of the genome. CpG
419 islands are usually associated with methylation and are known to regulate gene
420 expression (Gardiner-Garden & Frommer 1987). We identified CpG islands using the CpG
421 island track within the UCSC Mouse Genome Browser (Haeussler *et al.* 2019; see
422 methods). While this initial analysis did not determine whether the CpG islands were
423 methylated or directly regulate gene expression, it highlighted the potential for gene
424 dysregulation when methylation patterns are altered. Compared to the genome, both up-
425 and down-regulated gene sets were less likely to contain intragenic CpG islands (22-30%
426 of DEGs compared of 55% of genes genome-wide, $p<0.005$; **Fig. 4A**). Moreover, down-
427 regulated DEGs were less frequently associated with proximal promoter CpG islands (26%
428 of DEGs, $p=0.025$) than both up-regulated DEGs and the genome (42% of genes; **Fig.**
429 **4A**). Overall, these findings suggested that genes that were differentially expressed after
430 blastocyst transfer were less likely to be cis-regulated by intragenic or proximal promoter
431 CpG methylation compared to the genome at large.

432 We identified 15 DEGs whose regulation was directly linked to CpG methylation at
433 specific genomic locations by other studies (**Table 5**). Based on the published data and
434 our RNA-seq results, we predicted that seven of these DEGs should be associated with

435 CpG hypomethylation and eight DEGs with CpG hypermethylation (**Table 5**). We sought to
436 test CpG methylation in two loci (e.g., *Prl3d1* promoter and the differentially methylated
437 region (DMR) associated with the *Rasgrf1* gene) via bisulfite pyrosequencing. Due to
438 tissue availability, bisulfite pyrosequencing was carried out on whole female placentas
439 (N=5 placentas from 3-4 litters/group), even though the RNA-sequencing experiment
440 assessed whole male placentas. To rectify potential sex differences, we first verified that
441 female placentas from transferred conceptuses showed similar dysregulation of DEGs as
442 male transferred conceptuses by performing qRT-PCR analysis. In all six DEGs assessed
443 (i.e., *Prl3d1*, *Rasgrf1*, *Dazl*, *Cldn11*, *Tfpi2*, *Eno2*), female and male transferred placentas
444 showed similar patterns of gene misexpression relative to same-sex controls (**Fig. 4B**).
445 Thus, regardless of sex, we expected CpG hypermethylation in the *Prl3d1* promoter
446 (Hayakawa *et al.* 2012) (**Fig. 4C**) in transferred placentas since *Prl3d1* mRNA expression
447 was low (**Fig. 2D, 4B**). Nevertheless, five CpG sites across the *Prl3d1* promoter revealed
448 comparable levels of methylation in non-transferred and transferred placenta groups (**Fig.**
449 **4D**). This methylation pattern was also similar to normal C57Bl/6N placentas without
450 decidua at E14.5 (Hayakawa *et al.* 2012) indicating that the presence of decidua in our
451 placentas was an unlikely confounder. Likewise, we assessed CpG methylation in the
452 *Rasgrf1* DMR (**Fig. 4C**). Reduced *Rasgrf1* mRNA expression in transferred placentas (**Fig.**
453 **2D, 4B**) intimated that hypomethylation of the *Rasgrf1* DMR was expected (Yoon *et al.*
454 2005). However, four out of five CpGs assessed showed similar levels of methylation in
455 transferred and control placentas (**Fig. 4E**). One CpG site in the *Rasgrf1* DMR (CpG-5)
456 was hypomethylated in transferred placentas (20.7 ± 4.1% methylated versus 38.6 ± 4.0%
457 methylated in controls; $p<0.0001$; **Fig. 4E**), but hypomethylation of a single CpG among
458 many is unlikely to be responsible for increased *Rasgrf1* mRNA expression. Altogether,
459 these data supported the hypothesis that disruption of DNA methylation at promoter
460 regions by blastocyst transfer might not lead to transcriptional changes in the mouse

 Accepted Manuscript published as REP-19-0293.R2. Accepted for publication: 18-Nov-2019

placenta at E10.5.

Some DEGs cluster in the genome implying common transcriptional regulation

Next, we determined the chromosomal location of DEGs (fold change >2) including 355 up-regulated and 188 down-regulated genes (**Fig. 5A**). While the DEGs were distributed throughout the genome, we observed several genomic clusters of two or more DEGs (**Fig. 5A**). Gene clustering was unlikely to occur by chance because no clusters were identified in a group of 60 randomly selected genes. This observation suggested that some DEGs might share common long-range, cis-acting regulatory mechanism(s). To explore this hypothesis further, we analysed a published data-set that defined enhancer-promoter units (EPUs) in C57Bl/6 placentas at term based on an active chromatin state at enhancers (i.e., enrichment for H3K4 monomethylation (me1) and H3K27 acetylation (ac)) and occupancy of RNA polymerase II at promoters (Shen *et al.* 2012). From this data, we predicted DEGs (fold change >2) that were coordinately regulated by cis-acting elements in the placenta based on their EPU co-localisation. A total of 33 EPUs were identified containing at least two DEGs and a maximum of eight DEGs (mean [± s.d.]: 2.6 ± 1.4 DEGs/EPU; **Fig. 5A-B, Supplementary table 4**). We found that 15.8% (86/543) of DEGs fell within shared EPUs and, in general, all DEGs within a single EPU showed a similar direction of misexpression (**Supplementary table 4**). This finding supported the hypothesis of shared long-range, cis-acting regulation of some DEGs and highlighted the potential importance of histone modifications in this process. Chromatin immunoprecipitation followed by DNA sequencing (ChIP-seq) will be required to explore whether blastocyst transfer affects histone modifications in the placenta.

DISCUSSION

Evidence suggests that ART might influence pregnancy outcome in an adverse manner, yet the mechanism is not well understood. Here we showed that blastocyst transfer after natural mating of healthy mice is sufficient to restrict placental growth at midgestation even though the associated embryos were of normal size, or even larger, on average. This phenotype corresponds with a placental transcriptome that was enriched for genes implicated in labyrinth formation, growth, vascular development, and transport function, and implies compensation by the placenta to increase its functional efficiency. Therefore, even minimal embryo manipulation by a technique used in all ART procedures has developmental implications for the placentation site and embryo. Our data suggest that changes in DNA methylation at proximal promoter regions might not disrupt gene expression in the placenta after blastocyst transfer. This is because DEGs were less likely to associate with CpG islands within a 20 kb region than genes in the genome at large and DNA methylation patterns remained unchanged in at least two DEG loci compared to non-transfer controls. The genomic clustering of some DEGs warrants further investigation of the effects of blastocyst transfer on long-range, cis-acting epigenetic mechanisms, including histone modifications and DNA methylation.

Fetal growth is contingent upon a functioning placenta since it is the interface between the maternal and fetal circulations, facilitating gas and metabolic exchange, and hormone production (Watson & Cross 2005). After blastocyst transfer, we observed placentas that were small at E10.5 suggesting delayed development and/or reduced placental growth. Since the associated embryos were of normal developmental stage and size, the placentas may have adjusted their functional performance to protect the embryo growth trajectory. To achieve this, the placenta might respond to fetal requirements by altering its structure, endocrine function, and/or nutrient transport capacity through transcriptional changes.

In the mouse, the labyrinth layer is the exchange barrier composed of a complex

 Accepted Manuscript published as REP-19-0293.R2. Accepted for publication: 18-Nov-2019

network of trophoblastic villi that separate the fetal capillaries from the maternal blood circulation (Watson & Cross 2005). We observed several genes associated with labyrinth formation that were up-regulated after blastocyst transfer including those involved in branching morphogenesis and vascularization as determined by genetic knockout mice (Sun *et al.* 1998, Xue *et al.* 1998, Liu & LeRoith 1999, Stumpo *et al.* 2004, Bell *et al.* 2006, Smith *et al.* 2006, Fotopoulou *et al.* 2010, Goyal *et al.* 2010, Perez-Garcia *et al.* 2018). These transcriptional changes might promote branching of additional villi and/or increased vascular density of existing villi (Wu *et al.* 2003) to improve the surface area for exchange. In support of this hypothesis, increased placental vascular density is apparent after IVF (together with embryo transfer) in bovine and ovine conceptuses (Miles *et al.* 2005, Grazul-Bilska *et al.* 2014). IVF followed by blastocyst transfer in mice might lead to increased branching morphogenesis since an initially small placenta at E12.5 develops into a large placenta by late gestation (Delle Piane *et al.* 2010, Bloise *et al.* 2012). To fully understand the effects of blastocyst transfer alone on mouse placental villus structure, a detailed morphological analysis is required. Additionally, it will be interesting to explore how specific transcriptional profiles relate to the morphological differences.

Alternatively, placentas are capable of stimulating nutrient transport to compensate for poor placental growth (Constancia *et al.* 2002). Similar to studies of whole mouse placentas at E15.5 after IVF without superovulation (Bloise *et al.* 2012), we observed many up-regulated genes in transferred placentas that encode for transport proteins (e.g., *Gjb1*, gap junction protein; *Slc7a9*, L-cystine transport; *Slc27a2*, fatty acid transport; *Slc7a11*, cysteine/glutamine transport; *Apom*, lipid transport, etc.) when compared to non-transferred controls. This implies functional compensation by a small placenta in response to fetal requirements. Placental transport assays (Constancia *et al.* 2002) will be required to more fully understand the degree to which transcriptional up-regulation leads to a functional increase in nutrient transport across the placenta. Furthermore, whether the

transferred placenta is able to continue to compensate in later stages of gestation as the demands by the fetus increase remains to be determined.

It is possible that blastocyst transfer affects other placental regions (e.g., junctional zone or decidua). For instance, we identified four placenta prolactin cluster genes (*Prl2c2*, *Prl3d1*, *Prl7a1*, *Prl8a1*), which are solely expressed in the spongiotrophoblast cells and TGC subtypes of the mouse placenta (Simmons *et al.* 2008) and were down-regulated in transferred placentas. Normally, the promoter of the *Prl3d1* gene (also known as *Pl1*) is hypomethylated in the mouse placenta compared to adult organs (Hayakawa *et al.* 2012). While DNA methylation was normal in the *Prl3d1* promoter of transferred placentas, it is possible that changes in histone modifications together with DNA methylation in a more broadly defined region surrounding the *Prl3d1* gene might be implicated. Further analysis of chromatin marks in this genomic region is required. Alternatively, reduced differentiation of progenitor cells within the ectoplacental cone of transferred conceptuses might lead to fewer parietal-TGCs (*Prl3d1*$^+$ cells) and/or spongtiotrophoblast cells (*Prl2c2*$^+$, *Prl7a1*$^+$, or *Prl8a1*$^+$ cells) at E10.5 and thus reduced expression of these genes would result. In support of this hypothesis, *Aldh3a1* and *Il33,* genes that regulate the differentiation and function of the progenitor cells within the ectoplacental cone (Nishiyama *et al.* 2015, Wang *et al.* 2017), were also down-regulated in transferred placentas. To better understand the effects of blastocyst transfer on trophoblast differentiation, a histological examination and systematic assessment of trophoblast marker gene expression is required. Regardless, altered expression of prolactin cluster genes might have implications for placenta morphology, metabolism, and hormone production (Simmons *et al.* 2008, Woods *et al.* 2018).

Many researchers studying the epigenetic effects of ART have performed directed analyses of imprinted regions in placentation sites from mid- to late gestation (reviewed by Choux *et al.* 2015) as a read-out of functional changes in genome-wide DNA methylation.

 Accepted Manuscript published as REP-19-0293.R2. Accepted for publication: 18-Nov-2019

565 Here, we performed a genome-wide approach to assess the placental transcriptome and
566 identified only three misexpressed genes associated with distinct imprinted control regions
567 (i.e., *Rasgrf1*, *Cobl*, *Tfpi2*) (Yoon *et al.* 2005, Monk *et al.* 2008, Shiura *et al.* 2009).
568 Therefore, unlike more invasive ART procedures, blastocyst transfer might not alter DNA
569 methylation to a great extent in the whole placenta at E10.5. Beyond imprinted genes and
570 in support of this hypothesis, fewer misexpressed genes in transferred placentas were
571 associated with intragenic and proximal promoter CpG islands than the rest of the genome
572 implicating long-range cis-acting epigenetic mechanisms. Furthermore, we showed that at
573 least two DEGs with known regulation by CpG methylation in the placenta (i.e., *Prl3d1* and
574 *Rasgrf1*) (Yoon *et al.* 2005, Hayakawa *et al.* 2012) displayed normal DNA methylation
575 patterns. A whole methylome analysis (e.g., whole genome bisulfite sequencing) will better
576 address whether blastocyst transfer alters DNA methylation in transferred placentas to
577 cause the widespread transcriptional changes.

578 Our data suggests that blastocyst transfer might disrupt other epigenetic
579 mechanisms, such as histone modifications. The effects of ART on histone modifications
580 are little studied and not well understood. Increased histone acetylation (e.g., H3K9ac,
581 H3K14ac) in mouse zygotes is associated with superovulation (Huffman *et al.* 2015).
582 Whether these changes are maintained by placenta cell lineages and influence gene
583 expression is unclear. While we did not assess the effects of blastocyst transfer on histone
584 modifications directly, we showed that some DEGs shared cis-acting regulatory elements
585 in the placenta, the identification of which was largely based on the enrichment of histone
586 modifications and RNA polymerase binding (Shen *et al.* 2012). As a result, these clustered
587 DEGs might be sensitive to regional changes in histone modifications at key stages of
588 development. Interestingly, four DEGs in transferred placentas (i.e., *AU022751*, *Myocd*,
589 *Chd5*, *Pygo1*) are regulators of histone modifications (Cao *et al.* 2005, Fiedler *et al.* 2008,
590 Potts *et al.* 2011, Zhuang *et al.* 2014, Maier *et al.* 2015, Kloet *et al.* 2016). Indeed, the

dysregulation of proteins involved in chromatin remodeling has implications for widespread transcriptional dysregulation beyond the EPUs identified. Therefore, our study sets the stage for future analyses including ChIP-seq experiments, which will be required to explore the effects of blastocyst transfer on the regulation of histone modifications.

How blastocyst transfer alters placental gene expression remains unclear. The establishment of epigenetic marks is initiated at the blastocyst stage (Hanna *et al.* 2018). Therefore, it is possible that the stress of a brief culture period, embryo handling, and/or placement into a new uterine environment during this key epigenetic milestone is sufficient to alter epigenetic marks and subsequent gene expression required for cells to differentiate and function. Since all ART require blastocyst transfer, it will be important to tease apart the transcriptional and developmental effects of the transfer process from the more invasive techniques. Furthermore, the ART field will benefit from epigenome-wide analyses of placentas derived from these technologies including DNA methylation together with histone modifications with the aim of looking beyond imprinted loci. This will allow for a holistic picture of the epigenetic framework that gives rise to transcriptional and functional changes in the placenta after ART, and thus the immediate and long-term effects on the fetus.

 Accepted Manuscript published as REP-19-0293.R2. Accepted for publication: 18-Nov-2019

DECLARATION OF INTEREST

Erica Watson is an Associate Editor of *Reproduction*. Erica Watson was not involved in the review or editorial process for this paper, on which she is listed as an author.

FUNDING

This work was supported by grants from the Centre for Trophoblast Research (CTR) (to EDW), Lister Institute for Preventative Medicine (to EDW), and Canadian Institutes for Health Research (to JCC). KM was funded by a Newnham College (Cambridge) studentship and A.G. Leventis scholarship. SJT was funded by a Next Generation Fellowship (CTR). GETB was funded by a Wellcome Trust PhD studentship in Developmental Mechanisms. RSH and MP were funded by the CTR.

AUTHOR CONTRIBUTION

EDW conceived the study. KM, RSH and EDW designed the experiments. RSH and MP performed the bioinformatic analysis. CGJ, KM, MP, SJT, GETB, and EDW performed experiments, analysed the data, and interpreted the results. EDW and JCC obtained funding. EDW and KM wrote the manuscript. All authors read and edited the manuscript.

ACKNOWLEDGEMENTS

RNA library preparation and sequencing was performed by Cambridge Genomic Services (Dept. Pathology, University of Cambridge).

REFERENCES

Agarwal R, Mori Y, Cheng Y, Jin Z, Olaru AV, Hamilton JP, David S, Selaru FM, Yang J, Abraham JM*, et al.* 2009 Silencing of claudin-11 is associated with increased invasiveness of gastric cancer cells. *PLoS One* **4** e8002.

Bell SE, Sanchez MJ, Spasic-Boskovic O, Santalucia T, Gambardella L, Burton GJ, Murphy JJ, Norton JD, Clark AR & Turner M 2006 The RNA binding protein Zfp36l1 is required for normal vascularisation and post-transcriptionally regulates VEGF expression. *Dev Dyn* **235** 3144-3155.

Bloise E, Lin W, Liu X, Simbulan R, Kolahi KS, Petraglia F, Maltepe E, Donjacour A & Rinaudo P 2012 Impaired placental nutrient transport in mice generated by in vitro fertilization. *Endocrinology* **153** 3457-3467.

Canovas S, Ross PJ, Kelsey G & Coy P 2017 DNA Methylation in Embryo Development: Epigenetic Impact of ART (Assisted Reproductive Technologies). *Bioessays* **39**.

Cao D, Wang Z, Zhang CL, Oh J, Xing W, Li S, Richardson JA, Wang DZ & Olson EN 2005 Modulation of smooth muscle gene expression by association of histone acetyltransferases and deacetylases with myocardin. *Mol Cell Biol* **25** 364-376.

Chen EY, Tan CM, Kou Y, Duan Q, Wang Z, Meirelles GV, Clark NR & Ma'ayan A 2013 Enrichr: interactive and collaborative HTML5 gene list enrichment analysis tool. *BMC Bioinformatics* **14** 128.

Choux C, Carmignac V, Bruno C, Sagot P, Vaiman D & Fauque P 2015 The placenta: phenotypic and epigenetic modifications induced by Assisted Reproductive Technologies throughout pregnancy. *Clin Epigenetics* **7** 87.

Chuma S & Nakatsuji N 2001 Autonomous transition into meiosis of mouse fetal germ cells in vitro and its inhibition by gp130-mediated signaling. *Dev Biol* **229** 468-479.

Constancia M, Hemberger M, Hughes J, Dean W, Ferguson-Smith A, Fundele R, Stewart F, Kelsey G, Fowden A, Sibley C*, et al.* 2002 Placental-specific IGF-II is a major modulator of placental and fetal growth. *Nature* **417** 945-948.

Delle Piane L, Lin W, Liu X, Donjacour A, Minasi P, Revelli A, Maltepe E & Rinaudo PF 2010 Effect of the method of conception and embryo transfer procedure on mid-gestation placenta and fetal development in an IVF mouse model. *Hum Reprod* **25** 2039-2046.

de Waal E, Mak W, Calhoun S, Stein P, Ord T, Krapp C, Coutifaris C, Schultz RM & Bartolomei MS 2014 In vitro culture increases the frequency of stochastic epigenetic errors at imprinted genes in placenta tissues from mouse concepti produced through assisted reproductive technologies. *Biol Reprod* **90** 1-12.

Dockery L, Gerfen J, Harview C, Rahn-Lee C, Horton R, Park Y & Davis TL 2009 Differential methylation persists at the mouse Rasgrf1 DMR in tissues displaying monoallelic and biallelic expression. *Epigenetics* **4** 241-247.

ENCODE Project Consortium 2012 An integrated encyclopedia of DNA elements in the human genome. *Nature* **489** 57-74.

European Society of Human Reproduction and Embryology (ESHRE), 2018 February 18. *ART Fact Sheet*. Retrieved from https://www.eshre.eu/. Grimbergen, Belgium.

Fauque P, Ripoche MA, Tost J, Journot L, Gabory A, Busato F, Le Digarcher A, Mondon F, Gut I, Jouannet P*, et al.* 2010 Modulation of imprinted gene network in placenta results in normal development of in vitro manipulated mouse embryos. *Hum Mol Genet* **19** 1779-1790.

Fiedler M, Sanchez-Barrena MJ, Nekrasov M, Mieszczanek J, Rybin V, Muller J, Evans P & Bienz M 2008 Decoding of methylated histone H3 tail by the Pygo-BCL9 Wnt signaling complex. *Mol Cell* **30** 507-518.

 Accepted Manuscript published as REP-19-0293.R2. Accepted for publication: 18-Nov-2019

Fortier AL, Lopes FL, Darricarrere N, Martel J & Trasler JM 2008 Superovulation alters the expression of imprinted genes in the midgestation mouse placenta. *Hum Mol Genet* **17** 1653-1665.

Fotopoulou S, Oikonomou N, Grigorieva E, Nikitopoulou I, Paparountas T, Thanassopoulou A, Zhao Z, Xu Y, Kontoyiannis DL, Remboutsika E*, et al.* 2010 ATX expression and LPA signalling are vital for the development of the nervous system. *Dev Biol* **339** 451-464.

Gonzalez TL, Sun T, Koeppel AF, Lee B, Wang ET, Farber CR, Rich SS, Sundheimer LW, Buttle RA, Chen YI*, et al.* 2018 Sex differences in the late first trimester human placenta transcriptome. *Biol Sex Differ* **9** 4.

Goyal R, Yellon SM, Longo LD & Mata-Greenwood E 2010 Placental gene expression in a rat 'model' of placental insufficiency. *Placenta* **31** 568-575.

Grazul-Bilska AT, Johnson ML, Borowicz PP, Bilski JJ, Cymbaluk T, Norberg S, Redmer DA & Reynolds LP 2014 Placental development during early pregnancy in sheep: effects of embryo origin on vascularization. *Reproduction* **147** 639-648.

Guller S, Buhimschi CS, Ma YY, Huang ST, Yang L, Kuczynski E, Zambrano E, Lockwood CJ & Buhimschi IA 2008 Placental expression of ceruloplasmin in pregnancies complicated by severe preeclampsia. *Lab Invest* **88** 1057-1067.

Guo XY, Liu XM, Jin L, Wang TT, Ullah K, Sheng JZ & Huang HF 2017 Cardiovascular and metabolic profiles of offspring conceived by assisted reproductive technologies: a systematic review and meta-analysis. *Fertil Steril* **107** 622-631 e625.

Haavaldsen C, Tanbo T & Eskild A 2012 Placental weight in singleton pregnancies with and without assisted reproductive technology: a population study of 536,567 pregnancies. *Hum Reprod* **27** 576-582.

Hackett JA, Reddington JP, Nestor CE, Dunican DS, Branco MR, Reichmann J, Reik W, Surani MA, Adams IR & Meehan RR 2012 Promoter DNA methylation couples genome-defence mechanisms to epigenetic reprogramming in the mouse germline. *Development* **139** 3623-3632.

Haeussler M, Zweig AS, Tyner C, Speir ML, Rosenbloom KR, Raney BJ, Lee CM, Lee BT, Hinrichs AS, Gonzalez JN*, et al.* 2019 The UCSC Genome Browser database: 2019 update. *Nucleic Acids Res* **47** D853-D858.

Han X, Wang R, Zhou Y, Fei L, Sun H, Lai S, Saadatpour A, Zhou Z, Chen H, Ye F*, et al.* 2018 Mapping the Mouse Cell Atlas by Microwell-Seq. *Cell* **172** 1091-1107 e1017.

Hanna CW, Demond H & Kelsey G 2018 Epigenetic regulation in development: is the mouse a good model for the human? *Hum Reprod Update* **24** 556-576.

Hayakawa K, Nakanishi MO, Ohgane J, Tanaka S, Hirosawa M, Soares MJ, Yagi S & Shiota K 2012 Bridging sequence diversity and tissue-specific expression by DNA methylation in genes of the mouse prolactin superfamily. *Mamm Genome* **23** 336-345.

Huffman SR, Pak Y & Rivera RM 2015 Superovulation induces alterations in the epigenome of zygotes, and results in differences in gene expression at the blastocyst stage in mice. *Mol Reprod Dev* **82** 207-217.

Ishikawa H, Seki R, Yokonishi S, Yamauchi T & Yokoyama K 2006 Relationship between fetal weight, placenta growth and litter size in mice from id- to late-gestation. *Reprod Toxicol* **21** 267-270.

Khosla S, Dean W, Brown D, Reik W & Feil R 2001 Culture of preimplantation mouse embryos affects fetal development and the expression of imprinted genes. *Biol Reprod* **64** 918-926.

Kloet SL, Makowski MM, Baymaz HI, van Voorthuijsen L, Karemaker ID, Santanach A, Jansen P, Di Croce L & Vermeulen M 2016 The dynamic interactome and

genomic targets of Polycomb complexes during stem-cell differentiation. *Nat Struct Mol Biol* **23** 682-690.

Kuleshov MV, Jones MR, Rouillard AD, Fernandez NF, Duan Q, Wang Z, Koplev S, Jenkins SL, Jagodnik KM, Lachmann A*, et al.* 2016 Enrichr: a comprehensive gene set enrichment analysis web server 2016 update. *Nucleic Acids Res* **44** W90-97.

Lee J, Oh JS & Cho C 2011 Impaired expansion of trophoblast spheroids cocultured with endometrial cells overexpressing cellular retinoic acid-binding protein 2. *Fertil Steril* **95** 2599-2601.

Liu H, Zhang Y, Gu HT, Feng QL, Liu JY, Zhou J & Yan F 2015 Association between assisted reproductive technology and cardiac alteration at age 5 years. *JAMA Pediatr* **169** 603-605.

Liu JL & LeRoith D 1999 Insulin-like growth factor I is essential for postnatal growth in response to growth hormone. *Endocrinology* **140** 5178-5184.

Maier VK, Feeney CM, Taylor JE, Creech AL, Qiao JW, Szanto A, Das PP, Chevrier N, Cifuentes-Rojas C, Orkin SH*, et al.* 2015 Functional Proteomic Analysis of Repressive Histone Methyltransferase Complexes Reveals ZNF518B as a G9A Regulator. *Mol Cell Proteomics* **14** 1435-1446.

Mann MR, Lee SS, Doherty AS, Verona RI, Nolen LD, Schultz RM & Bartolomei MS 2004 Selective loss of imprinting in the placenta following preimplantation development in culture. *Development* **131** 3727-3735.

Miles JR, Farin CE, Rodriguez KF, Alexander JE & Farin PW 2005 Effects of embryo culture on angiogenesis and morphometry of bovine placentas during early gestation. *Biol Reprod* **73** 663-671.

Monk D, Wagschal A, Arnaud P, Muller PS, Parker-Katiraee L, Bourc'his D, Scherer SW, Feil R, Stanier P & Moore GE 2008 Comparative analysis of human chromosome 7q21 and mouse proximal chromosome 6 reveals a placental-specific imprinted gene, TFPI2/Tfpi2, which requires EHMT2 and EED for allelic-silencing. *Genome Res* **18** 1270-1281.

Nishiyama M, Nita A, Yumimoto K & Nakayama KI 2015 FBXL12-Mediated Degradation of ALDH3 is Essential for Trophoblast Differentiation During Placental Development. *Stem Cells* **33** 3327-3340.

Orfanelli U, Wenke AK, Doglioni C, Russo V, Bosserhoff AK & Lavorgna G 2008 Identification of novel sense and antisense transcription at the TRPM2 locus in cancer. *Cell Res* **18** 1128-1140.

Ozler S, Oztas E, Guler BG, Pehlivan S, Kadioglu N, Ergin M, Uygur D & Danisman N 2016 Role of ADAMTS5 in Unexplained Fetal Growth Restriction (FGR). *Fetal Pediatr Pathol* **35** 220-230.

Padmanabhan N, Jia D, Geary-Joo C, Wu X, Ferguson-Smith AC, Fung E, Bieda MC, Snyder FF, Gravel RA, Cross JC*, et al.* 2013 Mutation in folate metabolism causes epigenetic instability and transgenerational effects on development. *Cell* **155** 81-93.

Perez-Garcia V, Fineberg E, Wilson R, Murray A, Mazzeo CI, Tudor C, Sienerth A, White JK, Tuck E, Ryder EJ*, et al.* 2018 Placentation defects are highly prevalent in embryonic lethal mouse mutants. *Nature* **555** 463-468.

Potts RC, Zhang P, Wurster AL, Precht P, Mughal MR, Wood WH, 3rd, Zhang Y, Becker KG, Mattson MP & Pazin MJ 2011 CHD5, a brain-specific paralog of Mi2 chromatin remodeling enzymes, regulates expression of neuronal genes. *PLoS One* **6** e24515.

Quinn M & Fujimoto V 2016 Racial and ethnic disparities in assisted reproductive technology access and outcomes. *Fertil Steril* **105** 1119-1123.

 Accepted Manuscript published as REP-19-0293.R2. Accepted for publication: 18-Nov-2019

780 **Rivera RM, Stein P, Weaver JR, Mager J, Schultz RM & Bartolomei MS** 2008
781 Manipulations of mouse embryos prior to implantation result in aberrant expression
782 of imprinted genes on day 9.5 of development. *Hum Mol Genet* **17** 1-14.
783 **Rouhi A, Lai CB, Cheng TP, Takei F, Yokoyama WM & Mager DL** 2009 Evidence for
784 high bi-allelic expression of activating Ly49 receptors. *Nucleic Acids Res* **37** 5331-
785 5342.
786 **Shen Y, Yue F, McCleary DF, Ye Z, Edsall L, Kuan S, Wagner U, Dixon J, Lee L,**
787 **Lobanenkov VV*, et al.*** 2012 A map of the cis-regulatory sequences in the mouse
788 genome. *Nature* **488** 116-120.
789 **Shiura H, Nakamura K, Hikichi T, Hino T, Oda K, Suzuki-Migishima R, Kohda T,**
790 **Kaneko-ishino T & Ishino F** 2009 Paternal deletion of Meg1/Grb10 DMR causes
791 maternalization of the Meg1/Grb10 cluster in mouse proximal Chromosome 11
792 leading to severe pre- and postnatal growth retardation. *Hum Mol Genet* **18** 1424-
793 1438.
794 **Simmons DG, Rawn S, Davies A, Hughes M & Cross JC** 2008 Spatial and temporal
795 expression of the 23 murine Prolactin/Placental Lactogen-related genes is not
796 associated with their position in the locus. *BMC Genomics* **9** 352.
797 **Smith BT, Mussell JC, Fleming PA, Barth JL, Spyropoulos DD, Cooley MA, Drake CJ**
798 **& Argraves WS** 2006 Targeted disruption of cubilin reveals essential
799 developmental roles in the structure and function of endoderm and in somite
800 formation. *BMC Dev Biol* **6** 30.
801 **Stumpo DJ, Byrd NA, Phillips RS, Ghosh S, Maronpot RR, Castranio T, Meyers EN,**
802 **Mishina Y & Blackshear PJ** 2004 Chorioallantoic fusion defects and embryonic
803 lethality resulting from disruption of Zfp36L1, a gene encoding a CCCH tandem zinc
804 finger protein of the Tristetraprolin family. *Mol Cell Biol* **24** 6445-6455.
805 **Sun WY, Witte DP, Degen JL, Colbert MC, Burkart MC, Holmback K, Xiao Q, Bugge**
806 **TH & Degen SJ** 1998 Prothrombin deficiency results in embryonic and neonatal
807 lethality in mice. *Proc Natl Acad Sci U S A* **95** 7597-7602.
808 **Tararbit K, Lelong N, Thieulin AC, Houyel L, Bonnet D, Goffinet F, Khoshnood B &**
809 **Group ES** 2013 The risk for four specific congenital heart defects associated with
810 assisted reproductive techniques: a population-based evaluation. *Hum Reprod* **28**
811 367-374.
812 **Thomopoulos C, Tsioufis C, Michalopoulou H, Makris T, Papademetriou V &**
813 **Stefanadis C** 2013 Assisted reproductive technology and pregnancy-related
814 hypertensive complications: a systematic review. *J Hum Hypertens* **27** 148-157.
815 **Tunster SJ** 2017 Genetic sex determination of mice by simplex PCR. *Biol Sex Differ* **8** 31.
816 **Tunster SJ, Jensen AB & John RM** 2013 Imprinted genes in mouse placental
817 development and the regulation of fetal energy stores. *Reproduction* **145** R117-137.
818 **Ueda O, Yorozu K, Kamada N, Jishage K, Kawase Y, Toyoda Y & Suzuki H** 2003
819 Possible expansion of "Window of Implantation" in pseudopregnant mice: time of
820 implantation of embryos at different stages of development transferred into the
821 same recipient. *Biol Reprod* **69** 1085-1090.
822 **Valenzuela-Alcaraz B, Crispi F, Bijnens B, Cruz-Lemini M, Creus M, Sitges M,**
823 **Bartrons J, Civico S, Balasch J & Gratacos E** 2013 Assisted reproductive
824 technologies are associated with cardiovascular remodeling in utero that persists
825 postnatally. *Circulation* **128** 1442-1450.
826 **Wang H, Feng Y, Bao Z, Jiang C, Yan W, Wang Y, Zhang C, Liu Y, Zhang Q, Zhang**
827 **W*, et al.*** 2013a Epigenetic silencing of KAZALD1 confers a better prognosis and is
828 associated with malignant transformation/progression in glioma. *Oncol Rep* **30**
829 2089-2096.

Wang R, Lohr CV, Fischer K, Dashwood WM, Greenwood JA, Ho E, Williams DE, Ashktorab H, Dashwood MR & Dashwood RH 2013b Epigenetic inactivation of endothelin-2 and endothelin-3 in colon cancer. *Int J Cancer* **132** 1004-1012.

Wang XH, Liu W, Fan DX, Hu WT, Li MQ, Zhu XY & Jin LP 2017 IL33 restricts invasion and adhesion of trophoblast cell line JEG3 by downregulation of integrin alpha4beta1 and CD62L. *Mol Med Rep* **16** 3887-3893.

Wang Y, Fang Y, Zhang F, Xu M, Zhang J, Yan J, Ju W, Brown WT & Zhong N 2014 Hypermethylation of the enolase gene (ENO2) in autism. *Eur J Pediatr* **173** 1233-1244.

Wang Z, Xu L & He F 2010 Embryo vitrification affects the methylation of the *H19*/*Igf2* differentially methylated domain and the expression of *H19* and *Igf2*. Fertil Steril **93** 2729-2793.

Watson ED & Cross JC 2005 Development of structures and transport functions in the mouse placenta. *Physiology (Bethesda)* **20** 180-193.

Weinerman R, Ord T, Bartolomei MS, Coutifaris C & Mainigi M 2017 The superovulated environment, independent of embryo vitrification, results in low birthweight in a mouse model. *Biol Reprod* **97** 133-142.

Wilson SL, Blair JD, Hogg K, Langlois S, von Dadelszen P & Robinson WP 2015 Placental DNA methylation at term reflects maternal serum levels of INHA and FN1, but not PAPPA, early in pregnancy. *BMC Med Genet* **16** 111.

Woods L, Perez-Garcia V & Hemberger M 2018 Regulation of Placental Development and Its Impact on Fetal Growth-New Insights From Mouse Models. *Front Endocrinol (Lausanne)* **9** 570.

Wu L, de Bruin A, Saavedra HI, Starovic M, Trimboli A, Yang Y, Opavska J, Wilson P, Thompson JC, Ostrowski MC*, et al.* 2003 Extra-embryonic function of Rb is essential for embryonic development and viability. *Nature* **421** 942-947.

Xue J, Wu Q, Westfield LA, Tuley EA, Lu D, Zhang Q, Shim K, Zheng X & Sadler JE 1998 Incomplete embryonic lethality and fatal neonatal hemorrhage caused by prothrombin deficiency in mice. *Proc Natl Acad Sci U S A* **95** 7603-7607.

Ye J, Coulouris G, Zaretskaya I, Cutcutache I, Rozen S & Madden TL 2012 Primer-BLAST: a tool to design target-specific primers for polymerase chain reaction. *BMC Bioinformatics* **13** 134.

Yoon B, Herman H, Hu B, Park YJ, Lindroth A, Bell A, West AG, Chang Y, Stablewski A, Piel JC*, et al.* 2005 Rasgrf1 imprinting is regulated by a CTCF-dependent methylation-sensitive enhancer blocker. *Mol Cell Biol* **25** 11184-11190.

Yue F, Cheng Y, Breschi A, Vierstra J, Wu W, Ryba T, Sandstrom R, Ma Z, Davis C, Pope BD*, et al.* 2014 A comparative encyclopedia of DNA elements in the mouse genome. *Nature* **515** 355-364.

Yuen RK, Chen B, Blair JD, Robinson WP & Nelson DM 2013 Hypoxia alters the epigenetic profile in cultured human placental trophoblasts. *Epigenetics* **8** 192-202.

Zhuang T, Hess RA, Kolla V, Higashi M, Raabe TD & Brodeur GM 2014 CHD5 is required for spermiogenesis and chromatin condensation. *Mech Dev* **131** 35-46.

 Accepted Manuscript published as REP-19-0293.R2. Accepted for publication: 18-Nov-2019

FIGURE LEGENDS

Figure 1. Blastocyst transfer in mice results in small placentas with a potential for increased efficiency at E10.5. (**A**) Images of embryos and placentas from non-transferred and transferred conceptuses at E10.5. Embryonic phenotypes shown include phenotypically normal (PN), growth enhanced (GE), growth restricted (GR), and developmentally delayed (DD) as determined by crown-rump lengths and somite pair counts. Arrowhead indicates where the allantois (i.e., the umbilical cord) was attached to the placenta. Scale bars: 500 μm. (**B-E**) Graphs showing (**B**) embryo weights, (**C**) placenta weights, (**D**) embryo:placenta (E/P) weight ratios, and (**E**) embryo crown-rump (CR) lengths in all non-transferred (black circles) and transferred (white circles) conceptuses at E10.5. Values are shown for male (m) and female (f) conceptuses (N=17-43) and data is presented as mean ± standard deviation (SD). Independent t test, *p<0.05, ***p<0.001. (**F**) Frequency distribution curves of embryo CR lengths as determined by sex for non-transferred (black solid line) and transferred (grey solid line) embryos. Only embryos staged as E10.5 were considered. Black dotted lines indicate the mean crown-rump length for non-transferred embryos. Lengths that fall within the grey shading indicate conceptuses that are grossly phenotypically-normal (PN). Grey dotted lines indicate two SDs from the control mean. Crown-rump lengths that were greater than two SDs below the mean were considered GR and greater than two SDs above the mean were considered GE. (**G**) Linear regression analysis of litter size versus embryo CR length in control (black circles) and transferred (white circles) conceptuses. A line of best fit is indicated (dotted line). (**H-K**) Graphs showing parameters for PN conceptuses only including (**H**) embryo CR length, (**I**) embryo weight, (**J**) placenta weight, and (**K**) E/P weight ratios in non-transferred (black circles) and transferred (white circles) conceptuses. Data is presented as mean ± SD and is shown for male (m) and female (f) conceptuses (N=10-43 conceptuses). Independent t tests, p<0.05, ***p<0.001.

Figure 2. Blastocyst transfer causes differential gene expression in mouse placentas at E10.5. An RNA-seq analysis was performed on whole male placentas from non-transferred and transferred experimental groups. N=4 placentas from 3-4 litters per group were analysed. Placentas assessed via RNA-seq are labeled in panels A, B, and D with the placenta ID (non-transferred (NT) or transferred (T) followed by the sample number and letter ID indicating the litter). (**A**) Graphs plotting litter size versus placental weight of male and female non-transferred placentas (left panel) and transferred placentas (right panel). The line of best fit (grey dotted line) is indicated, and the p and R^2 values from a linear regression analysis are shown. Green and blue data points are samples used in the RNA-seq experiment. (**B**) Principal component analysis of the RNA-seq data of whole male placentas from control non-transferred (green circles) and transferred (blue circles) conceptuses. (**C**) MA plot revealing 543 differentially expressed genes (DEGs) with a fold change $>\log_2 1.0$ (i.e., fold change ≥2; $p<0.05$) in placentas from transferred conceptuses compared to non-transferred controls. 188 DEGs were down-regulated (blue) and 355 DEGs were up-regulated (red). (**D**) Heat map showing differential expression of selected DEGs in non-transferred (NT) and transferred (T) placentas. Scale shown is $\log_2$[fold change]. Red, gene up-regulation; green, gene down-regulation. (**E-F**) Validation of RNA-seq data by qRT-PCR analysis in independent placentas from non-transferred (black bars) and transferred (white bars) conceptuses. Data is presented as fold change compared to controls (normalised to 1). N=4-7 placentas per group from 2-4 litters. Graphs show qRT-PCR data of representative genes that were significantly (**E**) down-regulated or (**F**) up-regulated in transferred placentas. Unpaired t tests with Welch correction or Mann-Whitney tests where appropriate, §p=0.05, *p<0.05, **p<0.01, ***p<0.001.

 Accepted Manuscript published as REP-19-0293.R2. Accepted for publication: 18-Nov-2019

924 **Figure 3. Spatial expression and ontological analyses of DEGs identified in**
925 **placentas of transferred mouse conceptuses at E10.5.** (**A**) UpsetR plot summarizing
926 the predicted spatial expression of 79 DEGs in the mouse placentation site. Data was
927 largely obtained from a published single cell RNA-sequencing data set on whole mouse
928 placenta at E14.5 (Han *et al.* 2018). See also Supplementary table 3. Dark grey bars, up-
929 regulated DEGs; light grey bars, down-regulated DEGs; black circles indicate cell specific
930 expression; white circle indicate that expression was undetected. TB, trophoblast; Lab TB,
931 labyrinth trophoblast; EPC TB, ectoplacental cone trophoblast; FVE, fetal endothelial
932 vascular cells; PE/EC, parietal endoderm or endodermal cells; HPSC, hematopoietic stem
933 cells; FEC, fetal erythroid cell; Dec, decidua; uNK, uterine natural killer cell. (**B**) Gene
934 ontology term enrichment analysis for DEGs in placentas of transferred conceptuses. The
935 numbers of genes in each term are also given.
936
937 **Figure 4. Alteration of proximal promoter CpG methylation might not disrupt**
938 **transcriptional change in the mouse placenta after blastocyst transfer.** (**A**) The
939 percentage of the top 50 down-regulated DEGs (grey bars, FC >3.1) or up-regulated
940 DEGs (white bars, FC >6.7) after blastocyst transfer that associate with intragenic or
941 proximal promoter CpG repeats (within 20 kb region). The percentage of 50 randomly
942 selected genes is indicated as a proxy for the genome (black bars). Fisher's exact test,
943 *p<0.05, **p<0.01, ***p<0.001. (**B**) Validation of differential gene expression in male (m)
944 and female (f) placentas from non-transferred (black bars) and transferred (white bars)
945 conceptuses at E10.5. Data is presented as fold change compared to controls (normalised
946 to 1; mean ± sd). N=4-7 placentas/group from 3-4 litters. Independent *t* test. §p=0.05;
947 *p<0.05; **p<0.01; ***p<0.001. (**C**) Schematic drawings of the *Prl3d1* promoter and
948 *Rasgrf1* differentially methylated region (DMR). Modified from (Yoon *et al.* 2005,
949 Hayakawa *et al.* 2012). Open and closed circles represent unmethylated and methylated

CpG sites in placental tissue, respectively. a-d represent regions assessed by bisulfite pyrosequencing in *Prl3d1* promoter. (**D-E**) CpG site-specific methylation (mean ± se) in (**D**) the promoter region of the *Prl3d1* gene and (**E**) the *Rasgrf1* DMR as determined via bisulfite pyrosequencing of DNA from control (black squares) and transferred (white squares) female placentas at E10.5. N=5 placentas/group from 3-4 litters. Independent *t* tests when primers spanned a single CpG site (i.e., *Prl3d1*, regions a, b, d) and two-way ANOVA with Sidak's multiple comparisons test when primers spanned two or more CpG sites (i.e., *Prl3d1*, region c; *Rasgrf1* DMR). ***p<0.001.

Figure 5. Clustering of differentially expressed genes (DEGs) in the mouse genome suggests shared long-range, cis-acting regulatory regions. (**A**) Schematic karyoplot representing mouse chromosomes 1-19, X and Y indicating the location of DEGs (log_2[fold change] > 1) in whole placentas after embryo transfer as determined via RNA-sequencing. Red, up-regulated genes; blue, down-regulated genes. Peaks on the left-hand side of each chromosome represent the degree of gene density in that genomic region. Yellow arrowheads indicate enhancer-promoter units (EPUs) containing at least two DEGs. (**B-D**) A schematic representation of two neighbouring EPUs (yellow bars) on chromosome 4 including one EPU (right) that contains the DEGs *Edn2* and *Foxo6*. The level of misexpression of these genes is indicated by the respective red dots on a log_2[fold change] scale. Additional features include: chromosomal location of peaks of enrichment for placental histone modifications, such as H3K4me1 (purple peaks), H3K4me3 (red peaks), and H3K27ac (light green peaks) generated using published ChIP-seq data (Yue *et al.* 2014), CpG islands (CGIs; green lines) and genes (blue). Grey peaks indicate ChIP-seq input. See also Supplementary table 4.

 Accepted Manuscript published as REP-19-0293.R2. Accepted for publication: 18-Nov-2019

Table 1. Embryonic phenotypes before and after blastocyst transfer in mice.

Recipient Female ID	Phenotype at E3.5 before transfer				No. of conceptuses at E10.5 (Implantation rate [%])	Phenotype at E10.5 after transfer					
	No. of embryos transferred	Blasto-cyst stage	Morula stage	Abnormal		PN	GE	GR	DD	CM	R
C57-T1	10	5	4	1	6 (60.0%)	3	1	0	0	0	2
C57-T2	9	6	3	0	0	-	-	-	-	-	-
C57-T3	10	3	7	0	6 (60.0%)	5	0	0	0	0	1
C57-T4	8	4	4	0	4 (50.0%)	0	0	0	4	0	0
C57-T5	10	4	3	3	6 (60.0%)	6	0	0	0	0	0
C57-T6	9	7	2	0	3 (33.3%)	0	1	1	0	0	1
C57-T7	8	7	1	0	5 (71.4%)	3	0	1	0	0	1
C57-T8	9	5	4	0	0	-	-	-	-	-	-
C57-T9	8	7	1	0	7 (87.5%)	5	1	0	0	0	1
C57-T10	10	6	4	0	6 (60.0%)	3	0	0	0	0	3
Total	**91**	**48**	**29**	**4**	**43 (47.2%)**	**25**	**3**	**2**	**4**	**0**	**9**

E, embryonic day; PN, phenotypically normal; GR, growth restricted; GE, growth enhanced; DD, developmentally delayed; CM, congenital malformation; R, resorption.

Table 2. Phenotypic comparison of non-transferred and transferred mouse conceptuses at E10.5

	C57Bl/6 non-transferred[a]	C57Bl/6 transferred[a]
Experimental group		
No. of conceptuses assessed at E10.5		
Total	95 (10 litters)	43 (8 litters)
Male	44 [b]	17 [b]
Female	45 [b]	17 [b]
Average No. of conceptuses/litter		
Total	9.5 ± 0.4	5.4 ± 0.5***
Male	4.4 ± 0.5 (46.5%) [b]	2.1 ± 0.5 (39.5%) [b]
Female	4.5 ± 0.4 (47.4%) [b]	2.1 ± 0.5 (39.5%) [b]
Phenotypes		
Phenotypically normal		
Total	8.6 ± 0.5 (90.5%)	3.1 ± 0.8*** (58.1%)
Male	4.2 ± 0.5 (95.5%)	1.3 ± 0.5*** (58.8%)
Female	4.1 ± 0.4 (91.1%)	1.9 ± 0.5*** (88.2%)
Growth enhanced		
Total	0.0	0.4 ± 0.2[c] (7.0%)
Male	0.0	0.4 ± 0.2[c] (17.6%)
Female	0.0	0.0
Growth restricted		
Total	0.4 ± 0.2 (4.2%)	0.3 ± 0.2 (4.7%)
Male	0.2 ± 0.1 (4.5%)	0.1 ± 0.1 (5.9%)
Female	0.2 ± 0.1 (4.4%)	0.1 ± 0.1 (5.9%)
Developmental delay		
Total	0.0	0.5± 0.5 (9.3%)
Male	0.0	0.4 ± 0.4 (17.6%)
Female	0.0	0.1 ± 0.1 (5.9%)
Congenital malformations		
Total	0.0	0.0
Male	0.0	0.0
Female	0.0	0.0
Resorptions[b]		
Total	0.5 ± 0.3 (5.3%)	1.1 ± 0.4 (20.9%)
Male	-	-
Female	-	-

[a]Data is presented as average number of conceptuses [± se] per litter unless otherwise indicated. Number in brackets indicates the percentage of total conceptuses with each phenotype.

[b]Resorptions could not be genotyped for sex due to maternal tissue contamination.

[c]p=0.08

 Accepted Manuscript published as REP-19-0293.R2. Accepted for publication: 18-Nov-2019

Table 3. Differentially expressed genes in placentas of transferred mouse conceptuses at E10.5 that are implicated in growth, placental phenotypes, and/or embryonic lethality

Gene	Gene function	Mouse knockout phenotype or clinical characteristics [timing of embryonic lethality]	Reference	FC
Genetic knockout or decreased expression: defective labyrinth, placental insufficiency and/or FGR				
Cubn	Receptor mediated endocytosis	Defects in chorioallantoic attachment [E10.5]	(Smith *et al.* 2006)	2.9
Enpp2	Angiogenesis	Defective chorioallantoic attachment [E10.5]	(Fotopoulou *et al.* 2010)	2.5
Zfp36l1	RNA binding protein	Failure of chorioallantoic attachment†, reduced branching morphogenesis in labyrinth layer, small spongiotrophoblast layer [E10.5†]	(Stumpo *et al.* 2004, Bell *et al.* 2006)	2.1
F2	Maintenance of vascular integrity	Reduced or absent branching morphogenesis in labyrinth layer [E10.5†]	(Sun *et al.* 1998, Xue *et al.* 1998)	3.4
Rpgrip1	Regulator of ciliary protein traffic	Abnormal vasculature in labyrinth at E14.5 ['Pre-weaning' lethality]	(Perez-Garcia *et al.* 2018)	-2.0
Slpi	Serine protease inhibitor	Down-regulated expression in rat model of placental insufficiency [ND]	(Goyal *et al.* 2010)	2.5
Igf1	Insulin-like growth factor	Severely growth restricted; unknown placental phenotype [Perinatal]	(Liu & LeRoith 1999)	2.2
Increased gene expression: trophoblast phenotype, placental insufficiency, preeclampsia, or FGR				
Aldh3a1	Aldehyde dehydrogenase	OE in mouse TSCs prevents differentiation into *Tpbpa*+ cells (EPC lineage) [ND]	(Nishiyama *et al.* 2015)	-9.3
Il33	Interleukin	Inhibits trophoblast invasion and adhesion in vitro [ND]	(Wang *et al.* 2017)	-4.0
Tac2	Disintegrin and metalloproteinase	Fetal growth restriction in humans associated with increased placental expression [ND]	(Ozler *et al.* 2016)	-3.1
Crabp2	Retinoic acid signaling pathway	OE in endometrial cell line causes decreased proliferation of trophoblast spheroids [ND]	(Lee *et al.* 2011)	2.3
Cp	Iron peroxidase	Increased placental expression associated with pre-eclampsia in humans [ND]	(Guller *et al.* 2008)	2.6
Slc9a2	Sodium/hydrogen exchanger	Up-regulated in rat model of placental insufficiency; unknown placental phenotype [Possible embryonic lethality†]	(Goyal *et al.* 2010)	2.9

†Incomplete penetrance; FC, fold change in RNA-sequencing experiment; OE, overexpression; E, embryonic day; ND, not determined; FGR, fetal growth restriction; TSCs, trophoblast stem cells; EPC, ectoplacental cone.

Table 4. Differentially expressed genes in placentas of transferred mouse conceptuses at E10.5 that encode for proteins with transporter function

Gene	Fold Change	Gene Function
Down-regulated genes		
Trpm2	-10.1	Calcium channel
Slc28a2l (Gm14085)	-5.15	Purine nucleoside transporter
Clca3a1	-3.90	Calcium-activated chloride channel
Slc17a8	-3.00	L-glutamate transporter
Ndufa4l2	-2.93	NADH dehydrogenase [ubiquinone], mitochondria
Slc28a2	-2.03	Sodium-coupled purine nucleoside transporter
Kcnab2	-2.03	Voltage-gated potassium channel, NADH oxidation
Up-regulated genes		
Kcnd2	5.13	Voltage-gated potassium channel
Kcne3	3.91	Voltage-gated potassium channel
Kcnj12	3.07	ATP-sensitive inward rectifier potassium channel
Atp6v1c2	2.89	Proton-exporting ATPase, phosphorylative mechanism
Slc9a2	2.87	Sodium/hydrogen exchanger
Slc13a5	2.87	Sodium-dependent citrate transporter
Gjb1	2.84	Gap junction protein
Slc7a9	2.72	Sodium-independent L-cystine transporter
Abcc6	2.68	ATP-binding cassette transporter
Cftr	2.62	ATP-gated chloride channel
Slc27a2	2.60	Fatty acid transporter
Hcn4	2.58	Cyclic nucleotide-gated potassium channel
Slc7a11	2.57	Cysteine/glutamine transporter
Cacna1b	2.56	Voltage-gated calcium channel
Jph2	2.42	Calcium channel
Slc39a8	2.31	Zinc ion transporter
Trpm3	2.31	Cation channel
Mttp	2.30	Microsomal triglygeride transfer protein
Kcnk2	2.21	Potassium channel
Asic2	2.14	Voltage-gated sodium channel
Apom	2.09	Lipid transport
Scnn1g	2.07	Amiloride-sensitive sodium channel
Amn	2.04	Cobalamin and lipid transport
Slc4a1	2.03	Chloride/bicarbonate exchanger

 Accepted Manuscript published as REP-19-0293.R2. Accepted for publication: 18-Nov-2019

Table 5. Differentially expressed genes in placentas from transferred mouse conceptuses at E10.5 with known regulation by DNA methylation

Gene name	Function	Known characteristics of epigenetically regulated expression	FC	Predicted CpG methylation*	Ref.
Down-regulated genes					
Trpm2	Cation channel	Methylation of inner CpG island: gene repression	-10.1	Hyper	(Orfanelli *et al.* 2008)
Klra4	Killer cell lectin-like receptor; cell adhesion	Promoter hypomethylation: gene activation	-8.8	Hyper	(Rouhi *et al.* 2009)
Dazl	RNA binding protein	Promoter methylation: gene repression	-5.0	Hyper	(Hackett *et al.* 2012)
Prl8a1	Prolactin hormone family	Placenta-specific promoter hypomethylation: gene activation	-2.9	Hyper	(Hayakawa *et al.* 2012)
Prl7a1	Prolactin hormone family	Placenta-specific promoter hypomethylation: gene activation	-2.9	Hyper	(Hayakawa *et al.* 2012)
Rasgrf1	Guanine nucleotide-releasing factor	(Imprinted) Paternally-inherited allele is methylated and biallelically expressed in the placenta; methylation leads to gene activation	-2.7	Hypo	(Yoon *et al.* 2005, Dockery *et al.* 2009)
Kazald1	Insulin growth factor binding protein family	Promoter hypomethylation: gene activation	-2.3	Hyper	(Wang *et al.* 2013a)
Prl3d1	Prolactin hormone family	Placenta-specific promoter hypomethylation: gene activation	-2.0	Hyper	(Hayakawa *et al.* 2012)
Up-regulated DEGs					
Edn2	Angiogenesis	Hypomethylation of intragenic region: gene activation	7.2	Hypo	(Wang *et al.* 2013b)
Cldn11	Gap junction protein	Promoter hypermethylation: gene repression	5.9	Hypo	(Agarwal *et al.* 2009)
Eno2	Glycolysis	Promoter hypermethylation: gene repression	5.7	Hypo	(Wang *et al.* 2014)
Inhba	TGFβ signaling pathway	Promoter hypermethylation in human placenta: gene repression	4.4	Hypo	(Wilson *et al.* 2015)
Cfb	Complement factor	Promoter hypermethylation: gene repression; in human placenta, promoter hypomethylated upon CytoT to SynT differentiation	4.4	Hypo	(Yuen *et al.* 2013)
Tfpi2	Serine protease	(Imprinted) Paternally-inherited allele is methylated at the ICR, maternally-inherited allele expressed the placenta	3.1	Hypo	(Monk *et al.* 2008)
Cobl	Actin interacting protein	(Imprinted) Tissue-specific parentally-biased expression; methylation on maternally-inherited allele at *Grb10* DMR in yolk sac results in *Cobl* expression from the maternal allele	2.6	Hyper	(Shiura *et al.* 2009)

*Predicted change in CpG methylation based on differential expression observed in RNA-sequencing experiment and published data. FC, fold change; ICR, imprinting control region; hypo, hypomethylated; hyper, hypermethylated; CytoT, cytotrophoblast; SynT, syncytiotrophoblast.

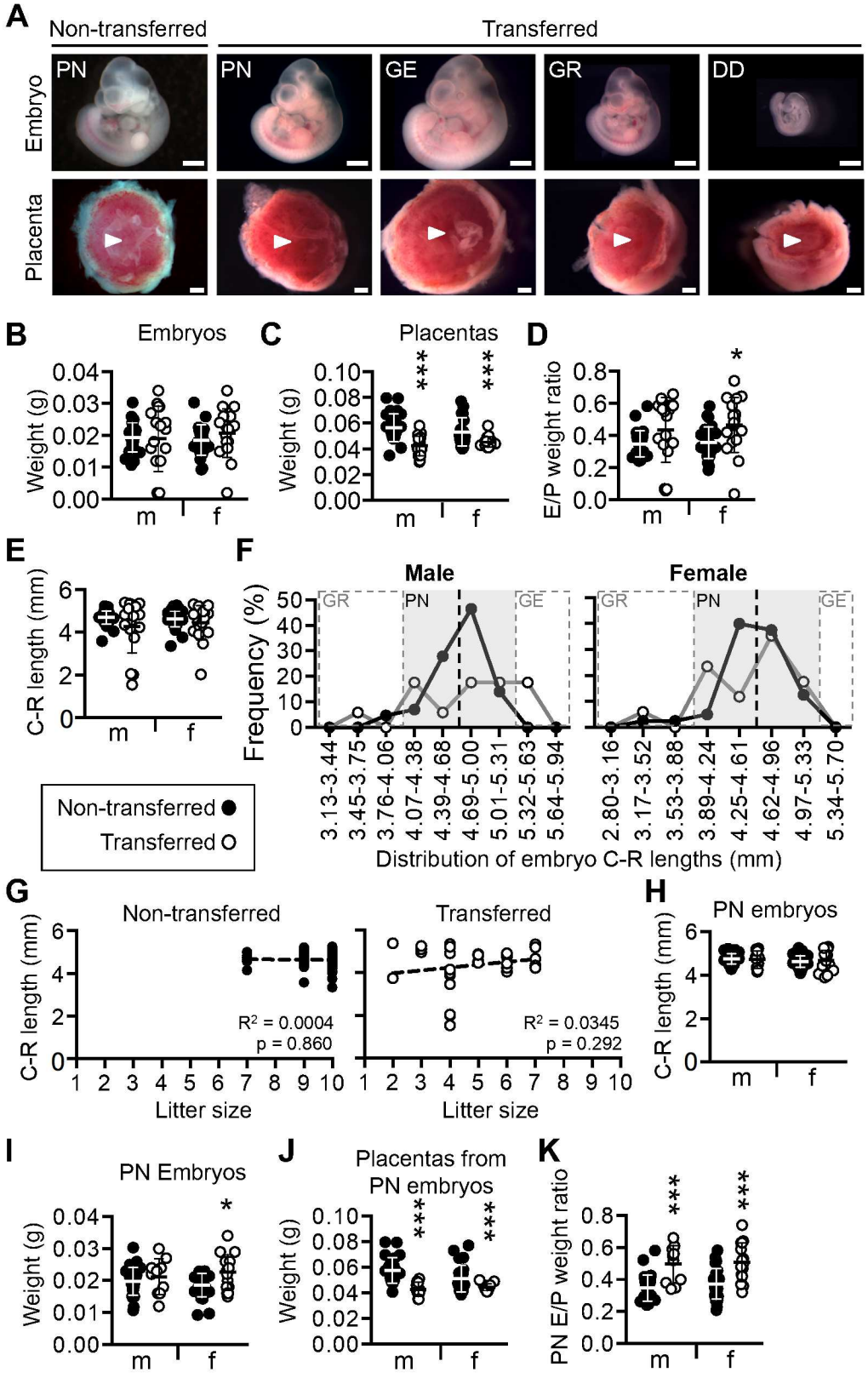

 Accepted Manuscript published as REP-19-0293.R2. Accepted for publication: 18-Nov-2019

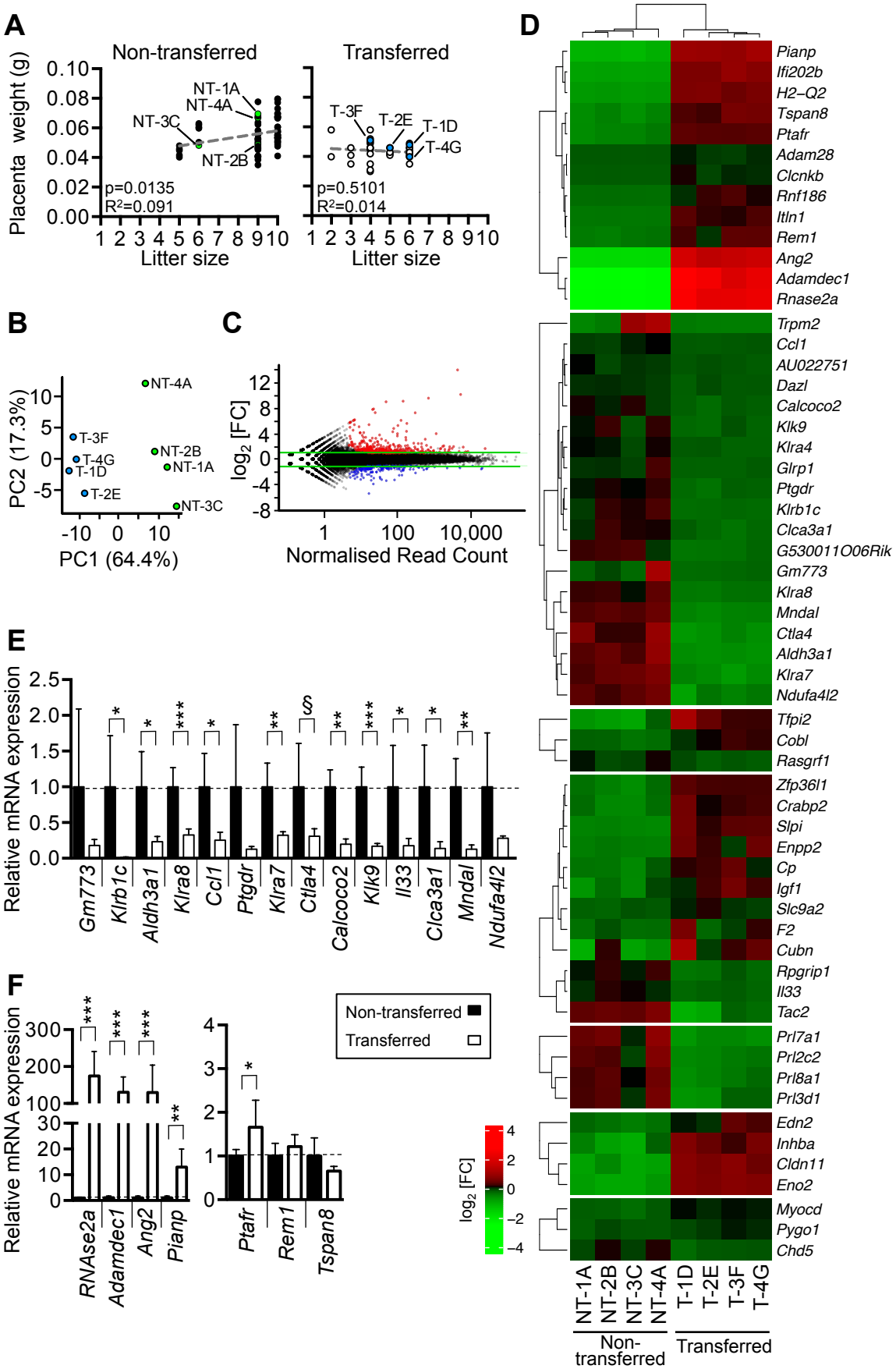

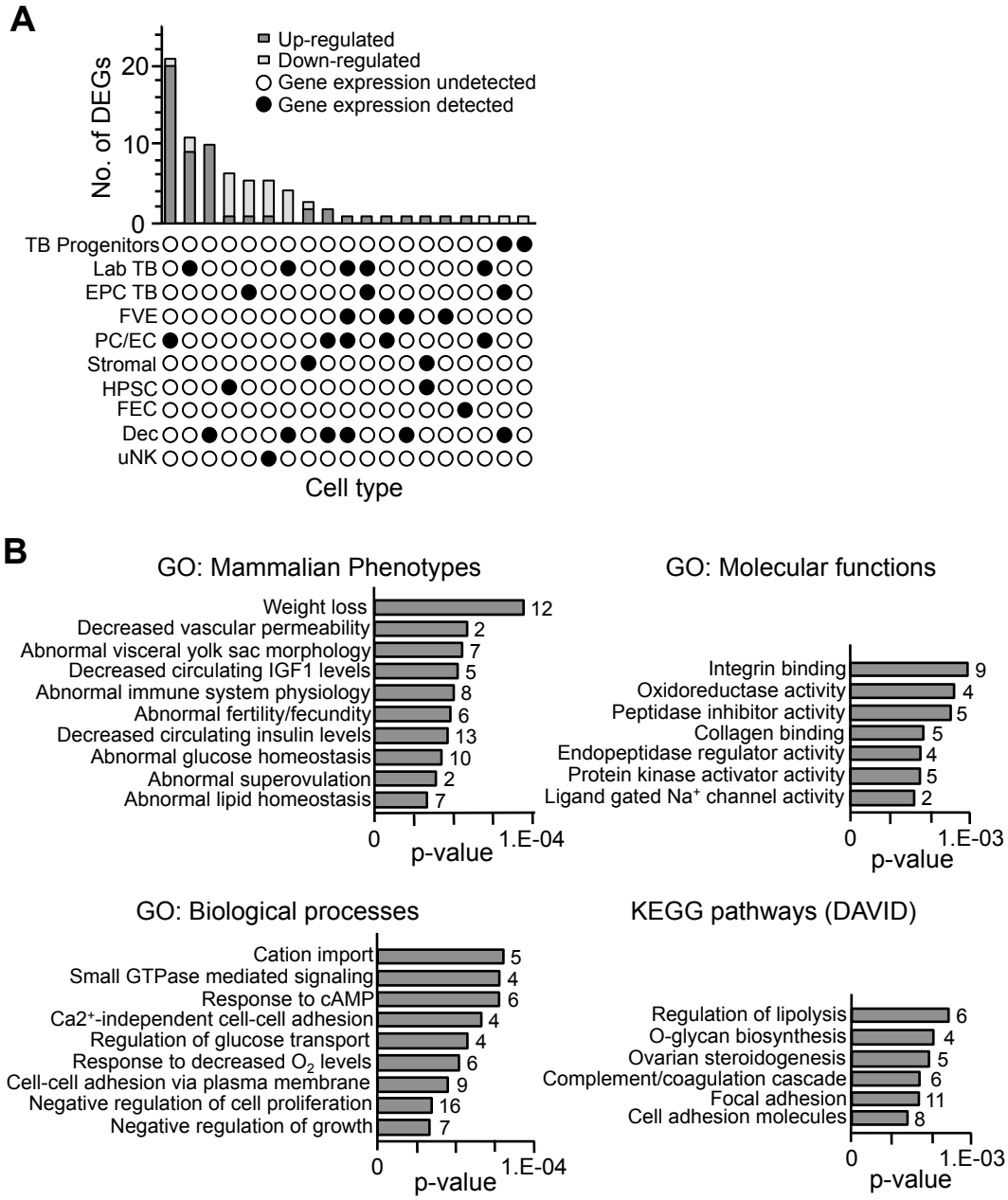

Accepted Manuscript published as REP-19-0293.R2. Accepted for publication: 18-Nov-2019

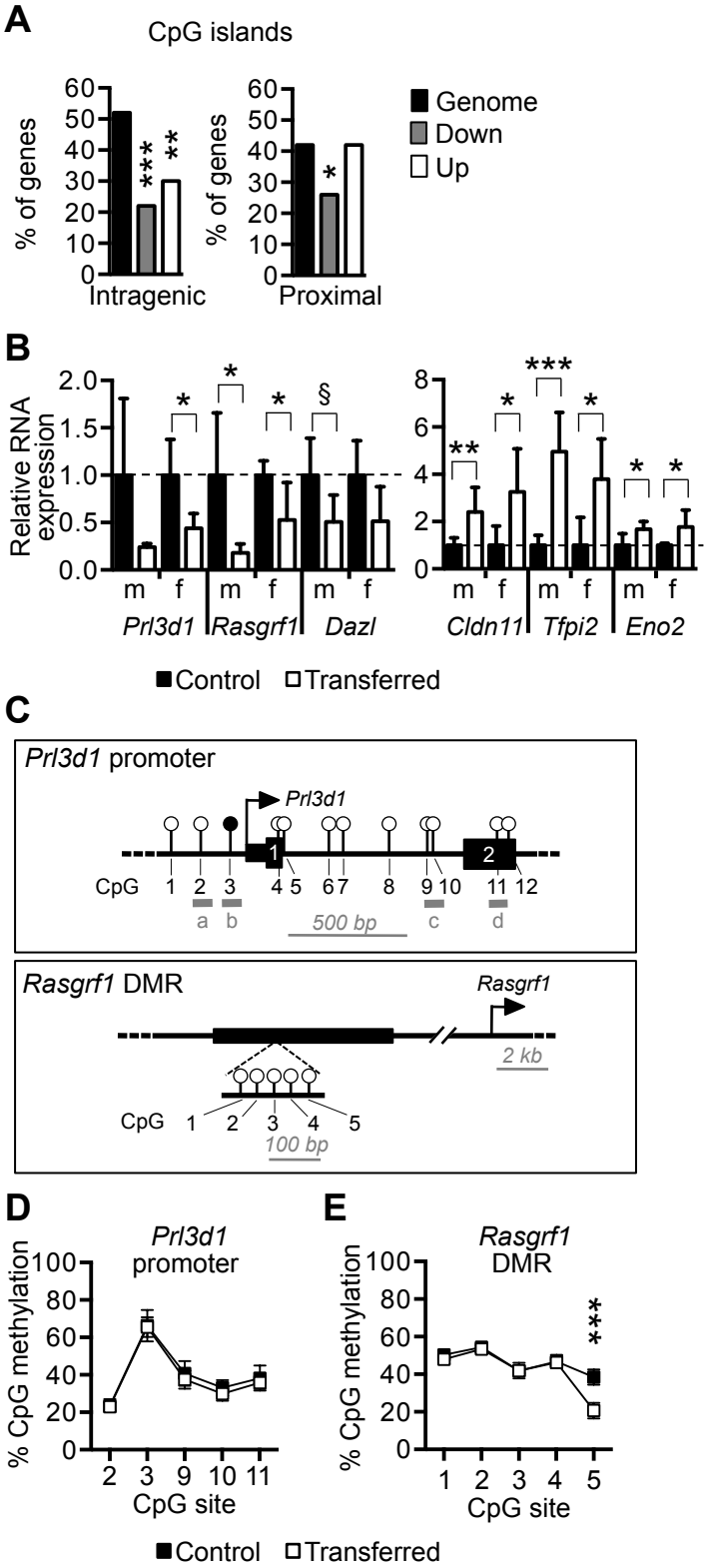

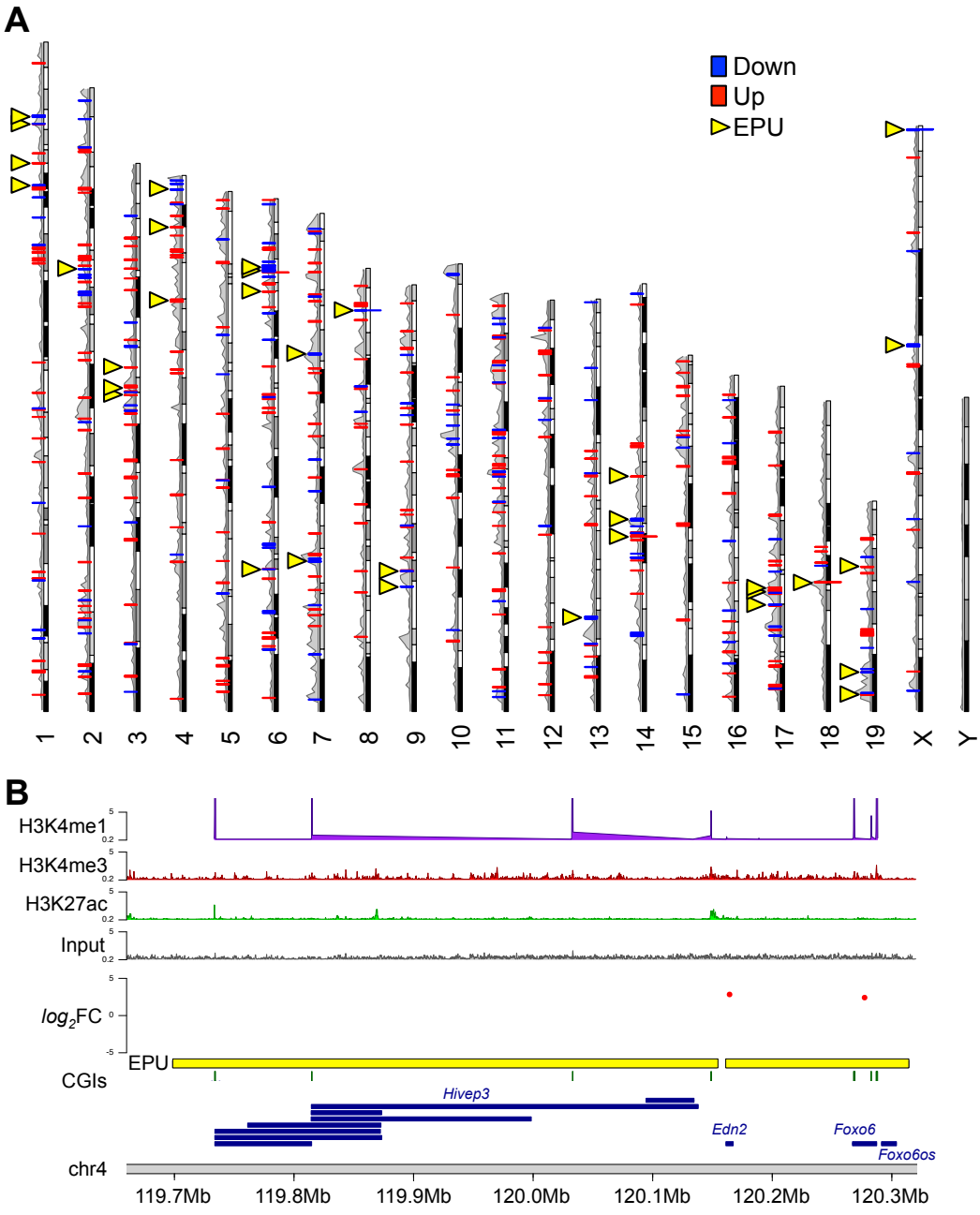

 Accepted Manuscript published as REP-19-0293.R2. Accepted for publication: 18-Nov-2019

1 **Supplementary Table 1**. Primer sequences (mouse)

RT-qPCR primers			
Mouse gene name	**Forward primer (5'→3')**	**Reverse primer (5'→3')**	**Ref.**
Adamdec1	GAGGGCTTGAGAACAACCAGA	GCCCCAGAAGATGCTTGGT	-
Aldh3a1	TCCTGCTCGAGATCTTCTCTTAC	GGAGGTGCCACATGACTTTAGG	(Nishiyama *et al.* 2015)
Ang2	GAAAGGAAGCCCTTATGGACGA	ATCTGAACCCTTTAGAGGCTCG	-
Calcoco2	GGCTGCTGTTCCTGGACTT	TCAGTGAGGGTGTAATAGCACAT	-
Ccl1	GACATTCGGCGGTTGCTCTA	GTAAGCATGCTCTTGCTGTCAAC	-
Clca3a1	ACCCCGAGGCAGAGTCTTT	CACATTGGTGCCAGTGATCC	-
Cldn11	TCCCCACCTGCCGAAAAATG	ACGTAGCCTGGAAGGATGAGG	-
Ctla4	CCATGCCCGGATTCTGACTT	GGACTTCTTTTCTTTAGCATCTTGC	-
Dazl	CTAGGCAGCCACCTCACGTA	GAAGTTGTGGCAGACATGATGG	-
Eno2	CCTGGAACTAAGGGATGGGG	GGTTGTCCAGTTTCTCCTGC	-
G530011O06Rik	TTTAGGCACAGGCATCGGAA	AGCATTTCGGTGAAGCAGGA	-
Gm773	TGGAAACTTAAGCCTGCATTTGT	TGCTGTAAGTGTAGAGTGTGCT	-
Il33	AACTCCAAGATTTCCCCGGC	TTATGGTGAGGCCAGAACGG	-
Klk9	GCTGGCCTCTTCTACCTCAC	GACCCACAGGTACGGCTTTC	-
Klra7	CTCTCCAATGAGTGTAAAAGTGCAA	AGCTTTGGGGGACCAGAGTA	-
Klra8	TTCTTCTTGGAGCCTCTTAGGG	AAAATATGTCCTGTGTCTCCACC	-
Klrb1c	GAGTGTCTTAGTGCGAGTCTTAGT	TTGTGGGCACTCTAAATTAACTGAA	-
Mndal	AAGTGGAGGGGAGTGGACAA	TTGGTGACCTTGATCTTGACGA	-
Ndufa4l2	TAAAAAGACACCCTGGGCTCAT	TGGGTTGTTCTTTCTGTCCCA	-
Pianp	CACCAGGCATGCAGTAAAGG	GAGCAGGTGGTAATACGGACA	-
Prl3d1	GGAGCCTACATTGTGGTGGA	CATTCCTGCGGAGCCTGAAA	-
Ptafr	TGAGCTCCTCCTACAGGCAT	TCGGAAAGAGCGTGTATCGAA	-
Ptgdr	CCTGCCTTTAATTTATCGTGCGT	GATGAAGATCCAGGGGTCCAC	-
Rasgrf1	CAAGAGGAGTGCGGACAACC	GCGCGCGTTTACAGATACTTC	-
RNAse2a	AGACTGGGAAACATGGGTCTGG	ATGCTGGATGTCAAACCACCG	-
Tfpi2	GCTCCGTTCTTGGTCTCACT	TAGAACTTGGGGATGAGGGC	-

Bisulfite pyrosequencing primers			
Location	**Forward primer**	**Reverse Primer**	**Sequencing primer**
Prl3d1 promoter: set a	[biotin]-TTAGATTATATGGGGGATATGTAGTATG	TCCTTAAAAATTATTAACATCCTCTTTACA	ACATCCTCTTTACATTTAAC
set b	TGTGTTAAATGTAAAGAGGATGTTAATAAT	[biotin]-ACCAAACTATACCTAAACCCA	AATGTTGTTTATTAATAGATATTGA
set c	TTGGAGTAAATGTATATTGTGAGATGT	[biotin]-ACAACAACAATTACATTCCTACTAT	AAATAAGTATTTTATTAAGTAATAG
set d	ATTGTTGTTGTTGGTGTTAAGT	[biotin]-CCAAAAACAAAAACATTACTTACAAATT	TGTTATGGTGTTTATTGAAG
Rasgrf1 DMR	GGGAAGATTATTAGTTGGGGAGGTG	[biotin]-CAACAAAAACCAAAATATCAATCCTAAC	ATTAGAGTTAAATATAAAGAATGG

2

3 All primers are listed in the 5' to 3' orientation

Supplementary Table 2. DEGs with known general expression in C57Bl/6 mouse placentas at term (Yue *et al.* 2014)

Gene name	FC	Gene function		Gene name	FC	Gene function
4930523C07Rik	2.59	Unknown, protein coding		*Jph2*	2.42	Junctional membrane complex protein
A2ml1	6.63	Peptidase inhibitor		*Kank4*	3.13	Cytoskeleton
Adamts5	2.76	Disintegrin and metalloproteinase		*Kazald1*	-2.25	Insulin-like growth factor binding
Adcy2	4.01	Adenylate cyclase		*Kcne3*	3.91	Potassium channel activity
Aff2	2.51	Transcriptional activator		*Klb*	3.97	FGF signaling pathway
Adgre1	2.03	G protein-coupled hormone receptor		*Klrd1*	-2.71	Killer cell lectin-like receptor; cell adhesion
Aldh1l2	-2.21	One-carbon metabolism (mitochondria)		*Krt23*	2.19	Intermediate filament
Apbb1ip	-2.13	Ras signaling pathway		*Kynu*	4.64	NAD cofactor biosynthesis
Apobec1	2.57	Cytodine deaminase		*Ltb4r1*	-2.71	G protein-coupled receptor activity
Arhgef26	2.37	Rho-guanine nucleotide exchange factor		*Lst1*	2.09	Membrane protein
Arsk	3.00	Sulfatase, hormone biosynthesis		*Mid1*	-2.27	Cytoskeleton
B3gat2	-2.55	Carbohydrate metabolism		*Mndal*	-2.96	RNA polymerase
Btg3	-2.86	Transcription factor binding protein		*Ms4a4b*	-3.71	Membrane protein
C1qtnf1	2.21	MAPK pathway		*Ms4a6c*	2.09	Membrane protein
Ccdc3	2.29	TNFα regulation		*Myocd*	3.61	Transcription factor
Cd53	-2.17	Integrin binding, involved in cell growth		*Naip6*	-2.17	Apoptosis inhibitory protein
Cmc4	-2.00	Mitochondrial protein import		*Ntrk1*	-2.32	Kinase in MAPK pathway
Chmp4c	3.89	Chromatin modifying protein, mitosis		*Osm*	-2.04	Secreted cytokine; growth regulator
Clca3a1	-3.90	Calcium-activated chloride channel		*Otoa*	-2.63	Predicted adhesion protein
Cldn1	3.30	Tight junction		*Pcdhga1*	2.52	Protocadherin
Cfb	4.40	Cell proliferation		*Pcdhgb7*	2.29	Protocadherin
Cobl	2.61	Actin nucleator		*Pianp*	50.8	Cell adhesion
Colgalt2	5.27	Extracellular matrix; PPARγ pathway		*Pllp*	2.37	Ion transport
Crabp2	2.32	Retinoic acid signaling pathway		*Ptafr*	4.85	G-protein coupled receptor activity
Csdc2	4.62	RNA-binding factor; histone synthesis		*Ptgs2*	-2.25	Prostaglandin synthesis
Ctla4	-5.52	Cytotoxic T-lymphocyte-associated protein		*Rai2*	2.00	Retinoic acid signaling pathway
Dpp4	2.32	Adenosine deaminase		*Rasgrf1*	-2.70	Ras protein signal transduction pathway
Efcab7	2.36	Hedgehog signalling		*Rgs1*	-4.34	Regulator of G protein signaling
Egln3	-2.45	HIF-1 signaling pathway		*Rnf150*	7.53	Ubiquitin protein ligase activity
Eno1b	4.73	Glycolysis		*Robo2*	3.41	Cell migration
Enpep	2.20	Aminopeptidase		*Schip1*	2.13	Estrogen metabolism
Fam20a	2.13	Unknown		*Slc7a11*	2.57	Cysteine and glutamate transport
Fam189a2	3.20	Unknown		*Slc9a2*	2.87	Na^+/H^+ transporter
Fam196a	3.89	Unknown		*Slc27a2*	2.60	Fatty acid transport
Far2	-2.03	fatty-acyl-CoA reductase		*Slc28a2*	-2.03	Na-coupled purine nucleoside

 Accepted Manuscript published as REP-19-0293.R2. Accepted for publication: 18-Nov-2019

		activity				transporter
Fbn1	2.38	Fibrillin		*Slit3*	2.32	Slit/Robo pathway
Galnt2	2.95	Glycosyltransferase		*Sorbs1*	2.28	Insulin signaling
Gpr19	2.46	G protein coupled receptor		*Spon1*	2.39	Cell adhesion
Gpr141	-2.27	Rhodopsin G protein-coupled receptor		*Stom*	2.12	Membrane protein
Gpr183	-3.60	G protein-coupled receptor		*Sytl3*	-2.53	Exocytosis
Grap2	2.32	GRB2-related adaptor protein		*Tfpi*	-2.57	Tissue factor pathway inhibitor
Gucy2c	-2.34	cGMP biosynthesis		*Thbs1*	2.15	Thrombospondin
Gxylt2	3.03	EGF pathway		*Thbs2*	2.69	Thrombospondin
Hipk2	2.19	Negative regulator of BMP pathway		*Trim5*	-2.01	E3 ubiquitin-ligase
Hkdc1	2.57	Glucose metabolism		*Trim55*	-2.37	Cytoskeleton
Hnf4a	2.66	Transcription factor		*Trpm2*	-10.1	Cation channel
Hspb7	16.7	Chaperone		*Tspan8*	3.46	Integrin binding
Ifi205	-2.15	Transcription factor		*Unc93a*	2.95	Unknown
Il15ra	-2.63	Interleukin		*Wdfy1*	2.67	Phosphatidylinositol 3-phosphate binding protein
Il33	4.04	Interleukin		*Wscd1*	3.07	Sulfotransferase activity
Itgb7	2.34	Integrin; cell-ECM adhesion		*Zfand4*	-2.19	Zinc finger protein

FC, fold change

Supplementary Table 3. DEGs with known spatial expression in mouse placentas

Gene name	FC	Gene function	Reported placental expression in mouse (stage of development)	Ref.
Expression in multiple cell types				
Cp	2.63	Iron homeostasis	Lab TB, SpA-TGC, FVE, PE, Dec (E14.5)	(Han *et al.* 2018)
Guca2b	4.67	cGMP biosynthesis	Lab TB (E14.5); Dec (E7.5)	(McConaha *et al.* 2011, Han *et al.* 2018)
Lcn2	3.34	Lipocalin 2	Lab TB (E14.5); Dec (E7.5)	(McConaha *et al.* 2011, Han *et al.* 2018)
Ltf	2.28	Lactotransferrin	Lab TB (E14.5); Dec (E7.5)	(McConaha *et al.* 2011, Han *et al.* 2018)
Tnfrsf11b	2.17	Tumor necrosis factor-receptor	Lab TB, Dec (E14.5)	(Han *et al.* 2018)
Gldn	-3.77	Extracellular matrix	Lab TB, PE (E14.5)	(Han *et al.* 2018)
Trpv6	3.68	Calcium transport	Lab TB (S-TGCs), EPC (GlyT) (E17.5)	(Yang *et al.* 2015)
Ang2	799.3	Ribonuclease	Lab TB (S-TGCs), FVE (E17.5)	(Geva *et al.* 2005)
Aldh3a1	-9.29	Aldehyde dehydrogenase	TS cells (in vitro), EPC (SpT) (E11.5-E17.5), Dec (E7.5)	(McConaha *et al.* 2011, Nishiyama *et al.* 2015)
Emp1	2.20	Cell adhesion	FVE, PE/EC (E14.5)	(Han *et al.* 2018)
Fabp4	2.15	Fatty acid binding protein	FVE, Dec (E12.5-E18.5)	(Makkar *et al.* 2014, Han *et al.* 2018)
Rnase4	4.43	Ribonuclease	PE/EC, Dec (E14.5)	(Han *et al.* 2018)
Zfp36l1	2.06	Zinc finger protein	Allantois, YS (E8.0-E9.5); Dec, (E14.5)	(Stumpo *et al.* 2004, Bell *et al.* 2006, Han *et al.* 2018)
Tmem26	3.20	Transmembrane protein	HPSC, Stromal cell (E14.5)	(Han *et al.* 2018)
Trophoblast progenitor cell only expression				
Gm1821	-2.31	Unknown; protein coding	Trophoblast progenitor (E14.5)	(Han *et al.* 2018)
Labyrinth trophoblast cells only expression				
Pigr	5.93	EGF pathway	Lab TB (E14.5)	(Han *et al.* 2018)
C3	4.60	Complement system; ERK1/2 cascade	Lab TB (E14.5)	(Han *et al.* 2018)
Sprr2f	4.09	Epidermis development	Lab TB (E14.5)	(Han *et al.* 2018)
Sftpd	3.91	Carbohydrate binding, superfactant homeostasis	Lab TB (E14.5)	(Han *et al.* 2018)
Fbln2	3.84	Extracellular matrix	Lab TB (E14.5)	(Han *et al.* 2018)
Prap1	3.35	Proline rich acidic protein	Lab TB (E14.5)	(Han *et al.* 2018)
Fermt1	3.12	Cell adhesion	Lab TB (E14.5)	(Han *et al.* 2018)
Robo1	2.90	Slit receptor, cell migration	S-TGCs (E13.5, E15.5)	(Li *et al.* 2015)
Srd5a1	-2.52	Steroid 5 α-reductase	Lab TB (E14.5)	(Han *et al.* 2018)
Napsa	-2.36	Aspartic protease	Lab TB (E14.5)	(Han *et al.* 2018)
Slc39a8	2.31	Zinc ion transporter	Lab TB (E14.5)	(Han *et al.* 2018)
EPC trophoblast lineage only expression				
Inhba	4.42	TGFβ signaling pathway	EPC, P-TGCs (E7.5)	(Albano *et al.* 1994)
Prl8a1	-2.89	Prolactin cluster	EPC, SpT, P-TGCs (E12.5-E18.5)	(Simmons *et al.* 2008, Han *et al.* 2018)
Prl7a1	-2.85	Prolactin cluster	EPC, SpT, P-TGCs (E8.5-E15.5)	(Simmons *et al.* 2008, Han *et al.* 2018)
Prl2c2	-2.27	Prolactin cluster (proliferin)	EPC, SpT, P-TGCs (E8.5-E18.5)	(Simmons *et al.* 2008)

 Accepted Manuscript published as REP-19-0293.R2. Accepted for publication: 18-Nov-2019

Prl3d1	-2.02	Prolactin cluster	P-TGCs (E8.5-E10.5)	(Simmons *et al.* 2008)
Fetal vascular endothelial (FVE) cell only expression				
Enpp2	2.48	Ectonucleotide pyrophosphatase/ phosphodiesterase	FVE (E14.5)	(Han *et al.* 2018)
Parietal endodermal (PE) cells and endodermal cells (EC) only expression				
H2-Q10	13.01	Cell adhesion, antigen processing	EC (E14.5)	(Han *et al.* 2018)
Edn2	7.15	Angiogenesis	PE (E14.5)	(Han *et al.* 2018)
Itih2	4.03	Serine protease; ECM stabilization	EC (E14.5)	(Han *et al.* 2018)
Ambp	4.01	Peptidase inhibitor	EC (E14.5)	(Han *et al.* 2018)
Apob	3.74	Apolipoprotein	EC (E14.5)	(Han *et al.* 2018)
Myl7	-3.71	Focal adhesions	PE (E14.5)	(Han *et al.* 2018)
Lrp2	3.43	Multi-ligand endocytic receptor	EC (E14.5)	(Han *et al.* 2018)
F2	3.37	Vascular integrity	EC (E14.5)	(Han *et al.* 2018)
Fbp2	3.25	Fructose bisphosphotase	PE (E14.5)	(Han *et al.* 2018)
Serpind1	3.07	Inhibitor of proteases	EC (E14.5)	(Han *et al.* 2018)
Cubn	2.89	Receptor mediating endocytosis	EC (E14.5)	(Han *et al.* 2018)
Gjb1	2.84	Gap junction protein	EC (E14.5)	(Han *et al.* 2018)
Slc7a9	2.72	Cysteine transport	EC (E14.5)	(Han *et al.* 2018)
Kng2	2.32	Kininogenin	EC (E14.5)	(Han *et al.* 2018)
Mttp	2.30	Lipoprotein assembly	EC (E14.5)	(Han *et al.* 2018)
Cldn2	2.29	Tight junction protein	EC (E14.5)	(Han *et al.* 2018)
Ang	2.21	Angiogenesis	PE, EC (E14.5)	(Han *et al.* 2018)
Aifm3	2.14	Oxidoreductase, apoptotic process	PE (E14.5)	(Han *et al.* 2018)
Apom	2.09	Apoplipoprotein	EC (E14.5)	(Han *et al.* 2018)
Sod3	2.08	Superoxide dismutase	EC (E14.5)	(Han *et al.* 2018)
Amn	2.04	Cobalamin transport	EC (E14.5)	(Han *et al.* 2018)
Ctsf	2.02	Cathepsin	PE (E14.5)	(Han *et al.* 2018)
Stromal cell only expression				
Sfrp2	2.84	WNT signaling pathway	Stromal cell (E14.5)	(Han *et al.* 2018)
Igf1	2.23	Insulin-like growth factor signaling	Stromal cell (E14.5)	(Han *et al.* 2018)
Fxyd1	-2.02	Ion channel protein	Stromal cell (E14.5)	(Han *et al.* 2018)
Hematopoietic stem cell (HPSC) only expression				
Gm14165	3.30	Unknown; pseudogene	HPSC (E14.5)	(Han *et al.* 2018)
Klk8	-3.25	Serine protease	HPSC (E14.5)	(Han *et al.* 2018)
Ifitm1	-2.83	Interferon induced transmembrane protein	HPSC (E14.5)	(Han *et al.* 2018)
Cd69	-2.13	Calcium and carbohydrate binding	HPSC (E14.5)	(Han *et al.* 2018)
Rps23	-2.06	Ribosomal protein	HPSC (E14.5)	(Han *et al.* 2018)
Mir703	-2.05	MicroRNA	HPSC (E14.5)	(Han *et al.* 2018)
Fetal erythroid cell only expression				
Slc4a1	2.03	Chloride/bicarbonate exchanger	Fetal erythroid cell (E14.5)	(Han *et al.* 2018)
Decidua (Dec) cell only expression				
Pdgfrl	14.46	PDGF receptor-like protein	Dec (E7.5)	(Ashley *et al.* 2010)
Fcgbp	9.67	Fc fragment of IgG binding protein	Dec (E7.5)	(McConaha *et al.* 2011)
Cldn11	5.87	Tight junction	Dec (E14.5)	(Han *et al.* 2018)

Sfrp5	4.15	WNT signaling pathway	Dec (E14.5)	(Han *et al.* 2018)
Cdo1	4.08	SHH co-receptor	Dec (E10.5, E14.5)	(Rakoczy *et al.* 2015, Han *et al.* 2018)
Erv3	3.27	Endogenous retrovial sequence	Dec (E7.5)	(McConaha *et al.* 2011)
Tfpi2	3.12	Serine protease involved in tissue remodelling	Dec (E14.5)	(Han *et al.* 2018)
Ear2	3.04	Ribonuclease	Dec (E7.5)	(McConaha *et al.* 2011)
Slpi	2.47	Serine protease inhibitor	Dec (E14.5)	(Han *et al.* 2018)
Aqp1	2.32	Aquaporin	Dec (E14.5)	(Han *et al.* 2018)
Uterine natural killer cell (uNK) expression				
Klrb1b	-3.27	Killer cell lectin-like receptor	uNK cells (14.5)	(Han *et al.* 2018)
Tff1	-2.75	Secreted protein	uNK cells (E14.5)	(Han *et al.* 2018)
Gzmn	-2.23	Endopeptidase	uNK cells (E14.5)	(Han *et al.* 2018)
Gzmb	-2.18	Hydrolyase	uNK cell (E14.5)	(Han *et al.* 2018)
Trbc1	2.00	T cell receptor	uNK cell (E14.5)	(Han *et al.* 2018)

Dec, decidua; E, embryonic day; EC, endodermal cell; ECM, extracellular matrix; EPC, ectoplacental cone; FC, fold change; FVE, fetal vascular endothelium; GlyT, glycogen trophoblast cell; HSPC, hematopoietic stem cell; Lab troph, undefined labyrinth trophoblast cell; PE, parietal endoderm; P-TGCs, parietal TGC; SMA cell, smooth muscle actin cell; SpT, spongiotrophoblast cells; SpA-TGC, spiral artery TGC; S-TGC, sinusoidal TGC; TGC, trophoblast giant cell; TS cell, trophoblast stem cell; YS, yolk sac.

References

Albano RM, Arkell R, Beddington RS & Smith JC 1994 Expression of inhibin subunits and follistatin during postimplantation mouse development: decidual expression of activin and expression of follistatin in primitive streak, somites and hindbrain. *Development* **120** 803-813.

Ashley RL, Henkes LE, Bouma GJ, Pru JK & Hansen TR 2010 Deletion of the Isg15 gene results in up-regulation of decidual cell survival genes and down-regulation of adhesion genes: implication for regulation by IL-1beta. *Endocrinology* **151** 4527-4536.

Bell SE, Sanchez MJ, Spasic-Boskovic O, Santalucia T, Gambardella L, Burton GJ, Murphy JJ, Norton JD, Clark AR & Turner M 2006 The RNA binding protein Zfp36l1 is required for normal vascularisation and post-transcriptionally regulates VEGF expression. *Dev Dyn* **235** 3144-3155.

Geva E, Ginzinger DG, Moore DH, 2nd, Ursell PC & Jaffe RB 2005 In utero angiopoietin-2 gene delivery remodels placental blood vessel phenotype: a murine model for studying placental angiogenesis. *Mol Hum Reprod* **11** 253-260.

Han X, Wang R, Zhou Y, Fei L, Sun H, Lai S, Saadatpour A, Zhou Z, Chen H, Ye F*, et al.* 2018 Mapping the Mouse Cell Atlas by Microwell-Seq. *Cell* **172** 1091-1107 e1017.

 Accepted Manuscript published as REP-19-0293.R2. Accepted for publication: 18-Nov-2019

Li P, Peng H, Lu WH, Shuai HL, Zha QB, Yeung CK, Li H, Wang LJ, Ho Lee KK, Zhu WJ*, et al.* 2015 Role of Slit2/Robo1 in trophoblast invasion and vascular remodeling during ectopic tubal pregnancy. *Placenta* **36** 1087-1094.

Makkar A, Mishima T, Chang G, Scifres C & Sadovsky Y 2014 Fatty acid binding protein-4 is expressed in the mouse placental labyrinth, yet is dispensable for placental triglyceride accumulation and fetal growth. *Placenta* **35** 802-807.

McConaha ME, Eckstrum K, An J, Steinle JJ & Bany BM 2011 Microarray assessment of the influence of the conceptus on gene expression in the mouse uterus during decidualization. *Reproduction* **141** 511-527.

Nishiyama M, Nita A, Yumimoto K & Nakayama KI 2015 FBXL12-Mediated Degradation of ALDH3 is Essential for Trophoblast Differentiation During Placental Development. *Stem Cells* **33** 3327-3340.

Rakoczy J, Lee S, Weerasekera SJ, Simmons DG & Dawson PA 2015 Placental and fetal cysteine dioxygenase gene expression in mouse gestation. *Placenta* **36** 956-959.

Simmons DG, Rawn S, Davies A, Hughes M & Cross JC 2008 Spatial and temporal expression of the 23 murine Prolactin/Placental Lactogen-related genes is not associated with their position in the locus. *BMC Genomics* **9** 352.

Stumpo DJ, Byrd NA, Phillips RS, Ghosh S, Maronpot RR, Castranio T, Meyers EN, Mishina Y & Blackshear PJ 2004 Chorioallantoic fusion defects and embryonic lethality resulting from disruption of Zfp36L1, a gene encoding a CCCH tandem zinc finger protein of the Tristetraprolin family. *Mol Cell Biol* **24** 6445-6455.

Yang H, Ahn C & Jeung EB 2015 Differential expression of calcium transport genes caused by COMT inhibition in the duodenum, kidney and placenta of pregnant mice. *Mol Cell Endocrinol* **401** 45-55.

Supplementary Table 4. Intersection of enhancer-promoter units (EPUs) and DEGs in mouse placentas of transferred conceptuses at E10.5.

EPU	chr	Gene name	ensembl_gene_id	FC	padj
EPU_1	chr1	*Gm15850*	ENSMUSG00000086264	2.06	0.044692317
		Gm26781	ENSMUSG00000097433	2.36	0.001894297
EPU_2	chr1	*4930523C07Rik*	ENSMUSG00000090394	2.59	6.00E-19
		Tnn	ENSMUSG00000026725	4.15	1.40E-07
EPU_3	chr1	*Itln1*	ENSMUSG00000038209	246.27	9.25E-12
		Ly9	ENSMUSG00000004707	2.04	0.004582751
EPU_4	chr1	*Ifi213*	ENSMUSG00000073491	2.70	6.65E-06
		Ifi208	ENSMUSG00000066677	3.95	3.73E-05
		Mndal	ENSMUSG00000090272	2.96	3.43E-33
		Ifi202b	ENSMUSG00000026535	40.50	4.86E-48
		Ifi205	ENSMUSG00000054203	2.15	0.009521903
EPU_5	chr2	*AI847159*	ENSMUSG00000084826	3.05	1.94E-11
		Gm14029	ENSMUSG00000086652	2.15	1.11E-16
EPU_6	chr3	*Sprr2f*	ENSMUSG00000050635	4.09	2.24E-73
		Sprr2g	ENSMUSG00000046203	5.19	8.43E-08
EPU_7	chr3	*Selenbp2*	ENSMUSG00000068877	11.23	3.30E-08
		Gm15264	ENSMUSG00000081355	11.02	6.06E-22
EPU_8	chr3	*Fam46c*	ENSMUSG00000044468	3.04	2.95E-246
		Gm12474	ENSMUSG00000053957	2.44	1.33E-05
EPU_9	chr4	*Edn2*	ENSMUSG00000028635	7.15	4.73E-06
		Foxo6	ENSMUSG00000052135	5.33	0.040654175
EPU_10	chr4	*Clcnkb*	ENSMUSG00000006216	75.48	0.019122743
		Hspb7	ENSMUSG00000006221	16.67	4.32E-48
EPU_11	chr4	*Chd5*	ENSMUSG00000005045	2.63	7.50E-42
		Kcnab2	ENSMUSG00000028931	2.02	1.06E-08
EPU_12	chr6	*Trbc1*	ENSMUSG00000076490	2.00	8.37E-49
		Trpv6	ENSMUSG00000029868	3.68	3.16E-13
EPU_13	chr6	*Aicda*	ENSMUSG00000040627	6.72	1.90E-08
		Apobec1	ENSMUSG00000040613	2.58	2.92E-10
EPU_14	chr6	*Klrb1c*	ENSMUSG00000030325	9.71	5.19E-16
		Klrb1b	ENSMUSG00000079298	3.27	6.46E-17
EPU_14	chr6	*Clec2i*	ENSMUSG00000030365	3.02	1.62E-48
		Klre1	ENSMUSG00000050241	2.63	0.017626571
EPU_15	chr6	*Klrd1*	ENSMUSG00000030165	2.71	0.001680801
		Klra4	ENSMUSG00000079852	8.83	2.84E-05
		Klra8	ENSMUSG00000089727	6.82	1.60E-46
		Klra14-ps	ENSMUSG00000072721	8.07	0.001104723
		Klra7	ENSMUSG00000067599	5.60	0.023579355
		Klra13-ps	ENSMUSG00000030178	2.87	2.64E-05
		Styk1	ENSMUSG00000032899	2.19	0.000660299
EPU_16	chr7	*Klk9*	ENSMUSG00000047884	4.07	0.022546162
		Klk8	ENSMUSG00000064023	3.25	0.047080871
EPU_17	chr7	*Trim5*	ENSMUSG00000060441	2.01	0.000295991
		Trim12a	ENSMUSG00000066258	2.14	6.65E-05
		Trim30d	ENSMUSG00000057596	2.04	7.85E-07

 Accepted Manuscript published as REP-19-0293.R2. Accepted for publication: 18-Nov-2019

EPU_18	chr8	*Bco1*	ENSMUSG00000031845	2.55	9.37E-07
		Gm20694	ENSMUSG00000093446	3.07	1.54E-21
EPU_19	chr9	*Gm7257*	ENSMUSG00000023093	7.67	0.01393948
		Gm9513	ENSMUSG00000090710	7.90	5.04E-08
EPU_20	chr9	*Jhy*	ENSMUSG00000032023	3.04	0.004658411
		Crtam	ENSMUSG00000032021	2.83	1.88E-06
EPU_21	chr13	*Prl8a1*	ENSMUSG00000019756	2.90	4.23E-11
		Prl7a1	ENSMUSG00000006488	2.85	0.008311304
EPU_22	chr14	*Rnase4*	ENSMUSG00000021876	4.43	1.62E-05
		Ang	ENSMUSG00000072115	2.21	7.06E-09
EPU_23	chr14	*Gzmn*	ENSMUSG00000015443	2.23	0.00522498
		Gzmb	ENSMUSG00000015437	2.18	0.006425581
EPU_24	chr14	*Adamdec1*	ENSMUSG00000022057	1194.78	4.01E-08
		Adam28	ENSMUSG00000014725	57.59	3.56E-09
EPU_25	chr17	*Tff1*	ENSMUSG00000024032	2.75	1.50E-24
		Ubash3a	ENSMUSG00000042345	2.01	0.022452667
EPU_26	chr17	*Lst1*	ENSMUSG00000073412	2.09	4.01E-05
		H2-Q1	ENSMUSG00000079507	16.56	2.96E-08
		H2-Q2	ENSMUSG00000091705	29.40	0.000132378
		H2-Q5	ENSMUSG00000055413	2.06	4.96E-13
		H2-Q10	ENSMUSG00000067235	13.01	0.001118777
		Cdsn	ENSMUSG00000039518	3.06	1.38E-25
EPU_27	chr17	*H2-T24*	ENSMUSG00000053835	2.69	0.014453217
		Gm11127	ENSMUSG00000079492	164.59	4.34E-10
		Gm8810	ENSMUSG00000091373	537.65	0.000572567
		Gm10499	ENSMUSG00000073403	573.81	2.17E-14
		Gm8909	ENSMUSG00000073402	70.98	0.000951945
EPU_28	chr18	*Pcdhga1*	ENSMUSG00000103144	2.52	1.05E-05
		Pcdhgb7	ENSMUSG00000104063	2.29	2.60E-06
EPU_29	chr19	*Ctsf*	ENSMUSG00000083282	2.02	6.71E-05
		Actn3	ENSMUSG00000006457	8.40	0.028619096
EPU_30	chr19	*Ms4a4b*	ENSMUSG00000056290	3.71	0.025157384
		Ms4a6c	ENSMUSG00000079419	2.09	0.018793207
EPU_31	chr19	*Sfrp5*	ENSMUSG00000018822	4.15	0.002602491
		Golga7b	ENSMUSG00000042532	2.41	0.035772232
EPU_32	chrX	*Gm5127*	ENSMUSG00000073010	4.69	0.026925397
		P2ry10	ENSMUSG00000050921	3.55	1.09E-05
		A630033H20Rik	ENSMUSG00000054293	2.11	0.046901925
EPU_33	chrX	*Mid1*	ENSMUSG00000035299	2.27	1.41E-05
		G530011O06Rik	ENSMUSG00000072844	14.49	1.93E-10
		Gm15726	ENSMUSG00000087263	4.86	0.002939615

See also Figure 5. Chr, chromosome; EPU, enhancer-promoter unit; FC, fold change.